AD_____

GRANT NUMBER DAMD17-94-J-4451

TITLE: Programmed Cell Death in Breast Cancer

PRINCIPAL INVESTIGATOR: Clark W. Distelhorst, M.D.

CONTRACTING ORGANIZATION: Case Western Reserve University
                           Cleveland, Ohio 44106

REPORT DATE: October 1998

TYPE OF REPORT: Final

PREPARED FOR: Commander
               U.S. Army Medical Research and Materiel Command
               Fort Detrick, Frederick, Maryland 21702-5012

DISTRIBUTION STATEMENT: Approved for public release;
                         distribution unlimited

The views, opinions and/or findings contained in this report are
those of the author(s) and should not be construed as an official
Department of the Army position, policy or decision unless so
designated by other documentation.

DTIC QUALITY INSPECTED 4

19990811 134

1

REPORT DOCUMENTATION PAGE

Form Approved
OMB No. 0704-0188

1. AGENCY USE ONLY *(Leave blank)*	2. REPORT DATE October 1998	3. REPORT TYPE AND DATES COVERED Final (1 Oct 94 - 30 Sep 98)	

4. TITLE AND SUBTITLE
Programmed Cell Death in Breast Cancer

5. FUNDING NUMBERS

DAMD17-94-J-4451

6. AUTHOR(S)
Clark W. Distelhorst, M.D.

7. PERFORMING ORGANIZATION NAME(S) AND ADDRESS(ES)
Case Western Reserve University
Cleveland, Ohio 44106

8. PERFORMING ORGANIZATION REPORT NUMBER

9. SPONSORING/MONITORING AGENCY NAME(S) AND ADDRESS(ES)
Commander
U.S. Army Medical Research and Materiel Command
Fort Detrick, Frederick, MD 21702-5012

10. SPONSORING/MONITORING AGENCY REPORT NUMBER

11. SUPPLEMENTARY NOTES

12a. DISTRIBUTION / AVAILABILITY STATEMENT

Approved for public release; distribution unlimited

12b. DISTRIBUTION CODE

13. ABSTRACT *(Maximum 200 words)*
Programmed cell death, or apoptosis, is a genetically regulated process through which a cell is active in bringing about its own death for the sake of the entire organism. Apoptosis is the mechanism by which the mammary gland normally undergoes involution. Also, apoptosis is the mechanism by which many cancer chemotherapeutic agents induce the death of breast cancer cells. This work has focused on the role of intracellular calcium as a mediator of the apoptotic process in the MCF-7 and MDA-MB-468 breast cancer cell lines. The findings indicate that release of calcium from intracellular stores by the calcium-ATPase inhibitor, thapsigargin, induces apoptosis in these cell lines. However, the cells mount an endogenous stress response that delays and inhibits the cell death response, so that the breast cancer cell lines are much less susceptible to thapsigargin-induced apoptosis than lymphoid cell lines, an observation that parallels the differential susceptibility of breast cancer and lymphomas to chemotherapy-induced cell death in vitro. One component of this work still in progress is to measure how the stress responses, and well know apoptosis inhibitors like Bcl-2, regulate intracellular calcium fluxes that mediate apoptosis. Ultimately, this work will provide new insight into the role of calcium in the apoptotic process in breast cancer cells and how the response of cells to apoptotic signals is regulated by endogenous stress responses.

14. SUBJECT TERMS Programmed Cell Death, Hormonal Regulation, Apoptosis, Thapsigargin, Calcium Signaling, Endoplasmic Reticulum, Breast Cancer

15. NUMBER OF PAGES
41

16. PRICE CODE

17. SECURITY CLASSIFICATION OF REPORT	18. SECURITY CLASSIFICATION OF THIS PAGE	19. SECURITY CLASSIFICATION OF ABSTRACT	20. LIMITATION OF ABSTRACT
Unclassified	Unclassified	Unclassified	Unlimited

NSN 7540-01-280-5500

Standard Form 298 (Rev. 2-89)
Prescribed by ANSI Std. Z39-18
298-102

FOREWORD

Opinions, interpretations, conclusions and recommendations are those of the author and are not necessarily endorsed by the U.S. Army.

_____ Where copyrighted material is quoted, permission has been obtained to use such material.

_____ Where material from documents designated for limited distribution is quoted, permission has been obtained to use the material.

_____ Citations of commercial organizations and trade names in this report do not constitute an official Department of Army endorsement or approval of the products or services of these organizations.

_____ In conducting research using animals, the investigator(s) adhered to the "Guide for the Care and Use of Laboratory Animals," prepared by the Committee on Care and use of Laboratory Animals of the Institute of Laboratory Resources, national Research Council (NIH Publication No. 86-23, Revised 1985).

_____ For the protection of human subjects, the investigator(s) adhered to policies of applicable Federal Law 45 CFR 46.

_____ In conducting research utilizing recombinant DNA technology, the investigator(s) adhered to current guidelines promulgated by the National Institutes of Health.

_____ In the conduct of research utilizing recombinant DNA, the investigator(s) adhered to the NIH Guidelines for Research Involving Recombinant DNA Molecules.

__√__ In the conduct of research involving hazardous organisms, the investigator(s) adhered to the CDC-NIH Guide for Biosafety in Microbiological and Biomedical Laboratories.

PI - Signature   Date

TABLE OF CONTENTS

A. INTRODUCTION

The purpose of the research conducted under DAMD17-94-J-4451 was to increase our understanding of the fundamental process of programmed cell death, or apoptosis, in breast cancer cells, and how this process involves intracellular calcium as a signaling agent. The following provides the background and rational for these studies.

What is programmed cell death (PCD), and why is it important? PCD, or apoptosis, is a naturally-occurring form of cell death important for the proper development and homeostasis of many tissues (1). For example, PCD is particularly prevalent in the immune system, where a large proportion of immature thymocytes are deleted through a process of negative selection and in the developing nervous system, where many neurons die soon after they are formed. PCD can be induced by a variety of different stimuli, including the deprivation of an essential growth factor or exposure to a cytotoxic signal from another cell. Classic examples of PCD include the death of immature lymphocytes induced by treatment with glucocorticosteroid hormones and the atrophy of prostatic tissue following androgen withdrawal. Regardless of the initiating factor, the single common denominator in all forms of PCD is that the cell is active in its own death, meaning that the cell kills itself by activating a genetically programmed suicide pathway.

PCD is an important physiological process that provides an efficient means of eliminating unwanted cells, both for development and for homeostasis. There is growing evidence that aberrant cell survival resulting from inhibition of PCD can lead to cancer (2). On the other hand, certain cancer treatments are based on the induction of PCD by hormonal manipulation (e.g., the treatment of lymphoid malignancies with glucocorticoids, the treatment of prostate cancer by androgen ablation).

What is the evidence that PCD occurs in breast cancer cells? The role of PCD in other malignancies, including lymphomas and prostate cancer, has received far more attention than the role of PCD in breast cancer. Recent studies, however, have established that PCD occurs both in the normal breast and in breast cancer cells under a variety of circumstances. Postlactation involution is a form of PCD in the normal breast (3), while regression of human breast cancer cells in nude mice following estrogen ablation is a form of PCD characterized by endonuclease activation, internucleosomal DNA fragmentation and enhanced expression of transforming growth factor ß (TGF-ß) and TRPM-2 genes (4). PCD can also be induced in breast cancer cells by treatment with the antiestrogen tamoxifen and the antiprogestin RU486 (5), or by treatment with the somatostatin analogue, SMS 201-995 (6).

A particularly important observation is that estrogen-independent human breast cancer cells that fail to undergo PCD in response to estrogen ablation, can be induced to undergo PCD by exposure to the fluorinated pyrimidines, 5-fluoro-2'-deoxyuridine or trifluorothymidine (7). Thus, the PCD pathway remains intact, at least in some breast cancer cells, even when it can no longer be triggered by estrogen ablation. This means that

5

it may be possible to develop new therapeutic strategies for breast cancer based on triggering PCD. However, before this can be accomplished, we need to develop a better understanding of the PCD pathway in breast cancer cells.

Why it is important to investigate the mechanism of PCD in breast cancer cells? Breast cancer is one of the most common, and often fatal, malignancies. Therefore, new therapeutic interventions are urgently needed. Although many breast cancers are initially responsive to endocrine manipulation (e.g., treatment with antiestrogens), most breast cancers eventually become hormone-independent. As noted above, however, even hormonally independent breast cancer cells can retain the major portion of the biochemical cascade involved in the PCD pathway (7). Therefore, one strategy for therapeutic intervention would be to develop methods for triggering this biochemical cascade. Before this can be done, however, we must gain a better understanding of the mechanism of PCD in breast cancer cells. To this end, the present proposal will characterize in detail changes in intracellular calcium homeostasis that accompany the PCD of breast cancer cells and will address the role of these changes in mediating PCD in breast cancer cells.

What is known about the mechanism of PCD? Much has been learned about the mechanism of PCD through studies in a variety of cell systems, but the PCD pathway has not been fully elucidated. Cells undergoing PCD undergo morphological changes referred to as "apoptosis". These changes include condensation of chromatin around the periphery of the nucleus, fragmentation of the nucleoli into coarse osmiophilic particles, dilation of the ER under the cell membrane, and contraction of the cytoplasm, while the mitochondria and other organelles appear unaffected. At a biochemical level, PCD is characteristically associated with activation of a constitutively expressed calcium-dependent endonuclease that cleaves the genome into fragments with lengths that are multiples of 180-base pairs, giving rise to a ladder pattern when DNA is analyzed by agarose gel electrophoresis. These characteristic morphological and biochemical changes distinguish PCD from other forms of cell death (e.g., toxic cell death) and have been demonstrated in breast cancer cells undergoing PCD in response to estrogen ablation (8,7).

An important concept is that PCD is a genetically programmed signal transduction pathway through which cells kill themselves. Elegant studies in the nematode *C. elegans* have defined genes that carry out various steps in the PCD pathway (1). A concept of considerable importance is that PCD is a physiologically regulated process that, along with cell proliferation, controls tissue homeostasis. In the nematode *C.elegans* induction of cell death by the *ced-3* and *ced-4* gene products can be inhibited by the product of the *ced-9* gene, while in mammals PCD can often be inhibited by expression of the *bcl-2* gene. In fact, the human *bcl-2* gene can complement a *ced-9* mutant.

The role of calcium in mediating PCD. There is considerable evidence that calcium is involved in the signal transduction pathway that mediates PCD in many types of cells, including lymphocytes, prostate cells and neuronal cells (reviewed in 9,10). The strongest

6

evidence for involvement of calcium in PCD has been derived using glucocorticoid-induced lymphocyte PCD as a model system. For example, treatment of immature lymphocytes with calcium ionophores induces PCD and elevations in cytoplasmic calcium concentration have been detected in glucocorticoid-treated thymocytes (10). Furthermore, glucocorticoid-induced PCD is accompanied by an early elevation of calmodulin mRNA and prevented by various manipulations suspected of interfering with calcium signaling, including pretreatment with a calmodulin inhibitor or an intracellular calcium chelator, and stable expression of a cDNA encoding the calcium-binding protein, calbindin.

There is also strong evidence that calcium is involved in tumor regression following hormonal ablation. For example, androgen withdrawal induces PCD of prostatic cancer cells, accompanied by endonuclease activation and DNA fragmentation believed to be the result of a sustained elevation of intracellular free calcium (4). Furthermore, regression of the normal prostate following androgen ablation is delayed by calcium channel blockers (11).

What our studies have contributed to understanding the role of calcium in PCD. Although there is strong evidence that calcium is involved in the PCD pathway, knowledge as to how the calcium signal is generated and how it mediates PCD has been totally lacking. Findings in this and other laboratories have provided considerable evidence that mobilization of calcium from an intracellular store located within the ER is involved in signaling apoptosis (12,13) and that BCL-2 inhibits apoptosis by interfering with ER calcium mobilization (14).

The ER is the major intracellular reservoir of calcium in nonmuscle cells, being far more important than the mitochondria in this regard (15). The ER plays a central role in intracellular signaling by sequestering and releasing "second messenger" calcium in response to a variety of agonists. In addition to providing a reservoir of calcium for use in intracellular signaling, the high calcium content of the ER lumen appears necessary for maintaining the structural and functional integrity of the ER, as well as other cellular functions including translation and cell division. ER calcium pool depletion can have a number of adverse effects on cells, including repression of protein synthesis and growth arrest. In response to ER calcium pool depletion, cells mount a self-protective response by inducing the synthesis of an hsp70 stress protein family member, GRP78 (16). GRP78 (also known as BiP) is one of a number of well characterized calcium-binding proteins that normally reside within the lumen of the ER. Along with its well characterized role in protein processing, GRP78 plays a role the cellular adaptation to conditions or treatments that cause a depletion of the ER calcium pool (16). Depletion of the ER calcium pool signals an increase in grp78 gene transcription, resulting in increased synthesis of GRP78, allowing protein synthesis to recover; whereas decreased expression of grp78 renders cells more susceptible to calcium ionophore induced growth arrest and cell death (16).

Our interest in the role of ER calcium in mediating apoptosis evolved directly from our

7

studies of the regulation of GRP78 synthesis in mouse lymphoma cells undergoing apoptosis in response to glucocorticoid treatment (17,18). Through these studies, which are part of a separate proposal submitted to the NIH, we have found that increased levels of GRP78 protect mouse lymphoma cells against glucocorticoid-induced apoptosis.

Intrigued by our findings regarding the effect of glucocorticoid treatment on GRP78 synthesis, we undertook a detailed investigation of the effect of glucocorticoid treatment on intracellular calcium homeostasis in WEHI7 mouse lymphoma cells (12). In response to glucocorticoid treatment, WEHI7 cells undergo apoptosis, with a classic pattern of internucleosomal DNA fragmentation detected within 6 hr of adding the glucocorticoid hormone dexamethasone. We found that a significant depletion of the ER calcium pool was detectable within 2-3 hr of adding dexamethasone. The ER calcium pool depletion was mediated through the glucocorticoid receptor and was temporally related to receptor-mediated transcriptional regulation, suggesting that glucocorticoid treatment might regulate the expression of gene(s) involved in the uptake or release of calcium from the ER. In glucocorticoid-treated cells, ER calcium pool depletion was accompanied by only a modest rise in cytosolic calcium concentration, and by a significant decrease in total cellular calcium, indicating that calcium mobilized from the ER in response to glucocorticoid treatment was actively pumped out of the cell through the plasma membrane. It is important to emphasize that ER calcium pool depletion was an early event in the apoptotic process that preceded loss of cell viability and onset of DNA fragmentation.

Interestingly, at the same time we were performing these studies, Dr. John Reed's laboratory was finding that withdrawal of IL-3 from an IL-3-dependent hematopoietic cell line induces apoptosis associated with a diminution of the ER calcium pool (19). Therefore, mobilization of ER calcium is not unique to apoptosis induction by glucocorticoids in lymphoid cells, but may be a common step in apoptosis induction in a variety of cells.

To investigate the cause-and-effect relationship between mobilization of ER calcium and apoptosis, we employed thapsigargin (TG), a highly selective and irreversible inhibitor of the ER associated calcium-ATPase which pumps calcium across a steep concentration gradient from the cytosol into the lumen of the ER. Because of a passive leak of calcium through the ER membrane, inhibition of calcium pumping by TG mobilizes calcium from the ER lumen, resulting in a sustained depletion of the ER calcium pool. Therefore, TG bypasses the glucocorticoid receptor pathway and acts directly at the level of the ER membrane to induce calcium release. We found that TG treatment induces apoptosis in WEHI7 cells; because of the highly selective nature of TG's action, this observation provided strong evidence of a cause-and-effect relationship between mobilization of ER calcium and apoptosis (14).

The findings of our research are evolving into a testable model of glucocorticoid-induced apoptosis. The initial step in this model involves the interaction of the glucocorticoid hormone with its receptor to form a hormone receptor complex that either enhances or

represses the transcription of unidentified genes, whose encoded protein acts either directly or indirectly to regulate ER calcium fluxes, resulting in a mobilization of ER calcium. The release of calcium into the cytosol could possibly alter the transcription of genes essential for normal cell growth and division, consistent with growing evidence of calcium-regulated transcription factors, or it could lead to activation of the constitutively expressed calcium, magnesium-dependent endonuclease, resulting in extensive DNA fragmentation. Alternatively, sustained depletion of the ER calcium pool could itself contribute to the apoptotic event. Depletion of the ER calcium pool has been shown to alter transcription of growth-related genes, induce a generalized repression of translation, and interfere with protein folding within the ER lumen. Therefore, depletion of the ER calcium pool might contribute to a loss of cell viability by interfering with the synthesis and processing of proteins required for normal cell division and viability. Furthermore, ER-associated calcium appears to be important for maintaining the structural integrity of the ER and, at least in certain cell types, a depletion of ER-associated calcium has a profound effect on the morphology of the ER, causing it to disperse and dissociate. Therefore, depletion of the ER calcium pool might contribute directly to apoptosis by disrupting ER structure and function. Interestingly, a recent report has suggested that the endogenous deoxyribonuclease involved in nuclear DNA degradation appears to be confined to the ER until it gains access to the nucleus during apoptosis (20). Perhaps depletion of the ER calcium pool triggers release of the endonuclease from the ER, allowing its entry into the nucleus.

In addition to providing novel insight into the role of calcium in signaling apoptosis, our studies have also contributed novel insight into the mechanism by which the BCL-2 oncogene opposes cell death. To investigate the possibility that the BCL-2 protein regulates calcium fluxes across the ER membrane, thereby preventing ER calcium mobilization and apoptosis, a human BCL-2 cDNA was introduced into the WEHI7.2 mouse lymphoma line and a series of clones stably expressing the BCL-2 mRNA and protein were isolated. We found that overexpression of BCL-2 interferes with glucocorticoid-induced growth inhibition and cell death in WEHI7.2 cells. Significantly, BCL-2 overexpression also interfered with TG-induced growth inhibition and cell death (14). Because the only known effect of TG at the cellular level is a potent and specific inhibition of ER-associated calcium pump activity, the observation that BCL-2 overexpression blocks TG-induced apoptosis suggests the possibility that the BCL-2 protein may function at the level of the ER membrane, interfering with calcium release and thereby preventing ER calcium pool depletion. Because of a passive leak in the ER membrane, inhibition of ER-associated calcium pumping by TG produces an immediate efflux of calcium from the ER lumen into the cytosol, resulting in a transient rise in cytosolic calcium concentration. We have found that the TG-induced rise in cytosolic calcium is significantly less in cells that express high levels of BCL-2 than in parental WEHI7.2 cells, indicating that the BCL-2 protein interferes with calcium movement through the ER membrane.

As another parameter of BCL-2's effect on ER-associated calcium fluxes, we measured the uptake of radioactive calcium into the ER of digitonin-permeabilized cells. Our findings

9

indicated that both the rate of calcium uptake and the total amount of calcium sequestered by the ER were greater in cells that express high levels of BCL-2 than in parental WEHI7.2 cells (21). Mitochondria function as a low affinity, high capacity calcium storage pool). To determine whether the BCL-2 protein selectively alters calcium uptake by the ER, or if BCL-2 also affects calcium uptake by mitochondria, radioactive calcium uptake measurements were performed at a high free calcium concentration (15 μM) in the absence of azide and in the presence of a reduced ATP concentration. Under these conditions, uptake of calcium was mainly into an azide sensitive, TG insensitive mitochondrial pool. Significantly, calcium uptake under these conditions was the same in cells that express high levels of BCL-2 and in parental WEHI7.2 cells, indicating that the rate of calcium uptake into mitochondria was unaffected by BCL-2 overexpression. In summary, our findings demonstrate for the first time that the antiapoptotic action of the BCL-2 oncoprotein is linked to a BCL-2 imposed alteration of ER calcium fluxes.

Summary. The fact that breast cancer cells can be induced to undergo PCD suggests that novel therapeutic strategies might be based on triggering the PCD pathway. However, this pathway must be understood first. Most of our current knowledge regarding the mechanism of PCD pertains to other cell systems and almost nothing is known about the mechanism of PCD in breast cancer cells. We have been gaining novel insight into the role of calcium in mediating PCD in mouse lymphoma cells. Now, in the present proposal, we will apply these insights and experimental approaches to elucidate the role of calcium in the PCD pathway of breast cancer cells.

B. BODY

B1. HYPOTHESIS/PURPOSE
The long term goal of the research conducted under DAMD17-94-J-4451 was to understand the programmed cell death (PCD) process in breast cancer cells so that new therapeutic strategies can be developed that utilize this pathway. The immediate goal was to investigate the role of calcium in mediating the PCD of breast cancer cells. The major hypothesis to be tested was that mobilization of calcium from an intracellular pool located within the ER triggers a cascade of biochemical events that produces apoptotic cell death, in response to both hormonal manipulation and treatment with the ER calcium pump inhibitor, thapsigargin.

B2. SPECIFIC AIMS (TECHNICAL OBJECTIVES)

Aim 1. Characterize in detail the alterations in intracellular calcium homeostasis associated with the PCD process in breast cancer cells.

Aim 2. Determine whether agents that specifically mobilize calcium from intracellular stores induce the PCD of breast cancer cells.

Aim 3. Determine whether measures that interfere with intracellular calcium fluxes

10

interfere with the PCD process in breast cancer cells.

Aim 4. Investigate the mechanism by which a PCD-related calcium signal is generated in breast cancer cells.

Aim 5. Investigate how intracellular calcium fluxes contribute to the PCD process in breast cancer cells.

B3. EXPERIMENTAL METHODS AND FINDINGS

The research accomplishments funded by DAMD17-94-J-4451 are reported here according to their fulfillment of the Statement of Work included with the original grant application.

Task 1, Develop model systems for studying PCD in breast cancer:

1a. MCF-7 and T47D breast cancer cell lines will be acquired and optimal culture conditions will be established. We systematically surveyed the current literature regarding available breast cancer cell lines, and also sought the advice of Dr. Gloria Heppner, Michigan Cancer Foundation. Our goal was to obtain cell lines which were reasonably well characterized and which were likely to serve as optimal models of apoptosis. Two cell lines were identified: MCF-7 and MB-MDA-468. These lines are well characterized and represent two ends of a spectrum: MCF-7 is a hormonally regulated line, which is known to express the antiapoptotic protein, Bcl-2; MB-MDA-468 is hormone independent and does not express detectable levels of Bcl-2. Although in the original proposal, we intended to also use the T47D line, after a detailed survey of the literature, we concluded that the MDA-MB-468 line would fulfill our aims better.

We obtained the MCF-7 line from Dr. Stanton Gerson's laboratory at CWRU, and the MB-MDA-468 line from Dr. Marc Lippman at Georgetown University. Specific culture conditions for maintaining optimal cell viability and growth were established, according to standard published methods (22). Cell viability was routinely monitored by measuring trypan blue dye exclusion (22). The amount of apoptosis under standard culture conditions was determined by fluorescence microscopy of ethidium bromide/acridine orange stained cells (22). On a routine basis, we observed in each cell line that dead cells, which generally have a clearcut apoptotic morphology, detach from the plastic tissue culture dish and float in the supernatant medium, whereas adherent cells are viable and do not show morphological signs of apoptosis. Under optimal culture conditions, the number of dead cells floating in the supernatant medium was less than 10% of the total cell population (attached cells plus detached cells). In the case of MCF-7 cells, we found it necessary to supplement the tissue culture medium with insulin; otherwise, viability and growth were not optimal.

In order to develop these cell lines as model systems for studying programmed cell death, it was necessary for us to characterize the cell lines in terms of their level of expression of

the antiapoptotic protein, Bcl-2, and for other members of the Bcl-2 family. Therefore, a Western blotting technique was set up to assess the level of Bcl-2 protein in MCF-7 and MB-MDA-468 cells. Methods of Western blotting have been described in earlier studies from this laboratory (14). Under conditions of exponential cell growth, Bcl-2 was not detected in MB-MDA-468 cells but was detected by Western blotting in MCF-7 cells (**Figure 1A**). The level of Bcl-2 increased following confluency of MDA-MB-468 cells, indicating that Bcl-2 expression may be affected by cell density (**Figure 1B**). To develop a panel of useful cell lines for investigating the role of Bcl-2 in breast cancer programmed cell death, we stably transfected MDA-MB-468 cells with a mammalian expression vector, pSFFV-Bcl-2, encoding human Bcl-2 cDNA, or control vector, pSFFV-neo, which does not encode Bcl-2. Methods for transfection and for preparation of plasmids has been described earlier by this laboratory (14). By Western blotting, we confirmed that the Bcl-2 transfectants did indeed express substantial levels of Bcl-2 protein, while control transfectants do not (**Figure 1C**). These cell lines were employed in subsequent experiments in this report.

Because the MCF-7 line is a hormonally responsive line, it was important for us to determine whether the level of Bcl-2 was affected by the hormonal milieu, as this could influence our studies of apoptosis in this experimental system. Therefore, we assessed the effect of estrogen withdrawal and supplementation on cell growth and the level of Bcl-2 in MCF-7 cells. To withdraw estrogen, cells were cultured in phenol red-free medium supplemented with charcoal stripped serum. (The charcoal stripping removes endogenous steroid hormones.) As shown in **Figure 2A**, culturing MCF-7 cells in medium supplemented with charcoal extracted serum (Ext Med) significantly repressed cell growth. We assessed Bcl-2 every 48 hr after placing cells in estrogen free medium. As shown in **Figure 2B & 2C**, the level of Bcl-2 declined over a period of 4-8 days following estrogen withdrawal. This was an important observation, as it suggested that the susceptibility of MCF-7 cells to programmed cell death might be influenced by the level of Bcl-2, which in turn was regulated by estrogen. The data in Figure 2 suggested that the decline in Bcl-2 expression occurring when cells were cultured in medium supplemented with charcoal stripped serum was due to estrogen withdrawal. An alternative hypothesis was that the decline in Bcl-2 was due to depletion of some other essential factor, other than estrogen, from the serum during charcoal extraction. To confirm that the decline in Bcl-2 was indeed due to estrogen withdrawal, we carried out the "add-back" experiments. In these experiments, MCF-7 cells were cultured in either regular medium or medium supplemented with charcoal extracted serum, in either the presence or absence of 1 nM 17ß-estradiol. After 6 days in culture, the Bcl-2 level was measured by Western blotting and expressed as fold induction (level of Bcl-2 + estradiol / level of Bcl-2 - estradiol) (**Figure 3**). The data indicate that estradiol indeed induces Bcl-2 expression, and that the level of Bcl-2 in cells cultured in medium supplemented with extracted serum was restored by supplementing the serum with 1 nM 17ß-estradiol. Hence, we conclude that the decline in Bcl-2 expression observed when cells are cultured in medium supplemented with charcoal extracted serum is, at least in large part, due to estrogen withdrawal. Moreover, consistent with the growth stimulatory effect of estrogen on MCF-7 cells, supplementation of charcoal

extracted serum with 1 nM 17ß-estradiol restored cell proliferation (**Figure 4**).

The data in **Figure 2** also indicate that the level of Bcl-2 increased approximately two-fold when cells were cultured for 8 days in the presence of unextracted serum. Thus, the data in **Figure 2** suggest that there is a correlation between cell proliferation and Bcl-2 expression. To test this correlation, independent of the influence of hormonal manipulations, we tested the relationship between cell proliferation and Bcl-2 expression in the hormone-independent MDA-MB-468 cell line. In **Figure 1, panel B**, the level of Bcl-2 in MDA-MB-468 cells was measured by Western blotting over a period of 4 days after cells reached confluency. Within 1 day of reaching confluency, Bcl-2 was readily detectable in the cells, whereas Bcl-2 was not detected during exponential growth. These data, coupled to those described in Figure 2, indicate that Bcl-2 expression correlates directly with cell density, suggesting that Bcl-2 expression may be regulated by cell-cell contact or by autocrine factors which increase with increased cell density.

In summary, two well characterized human breast cancer cell lines were identified for use in our work. One cell line, MCF-7 was found to express Bcl-2 in an estrogen-regulated fashion. The other cell line, MB-MDA-468, was found to express Bcl-2 when allowed to remain at confluence, but not during exponential growth.

1b. Methods of inducing PCD will be established, using both hormonal and non-hormonal manipulations. 1c. PCD assays, including DNA fragmentation assays, will be applied to breast cancer cells undergoing PCD. To determine whether or not estrogen withdrawal induces apoptosis in MCF-7 cells, we cultured the cells in the presence of charcoal-extracted serum for up to 8 days. This corresponds to the time period over which we characterized Bcl-2 expression and cell growth. Cells were stained with ethidium bromide and acridine orange and then examined for apoptotic morphology by fluorescence microscopy, using previously published methods (22). No morphological evidence of apoptosis was observed. Furthermore, we analyzed cellular DNA derived from cells at various time points, up to 8 days during culture in charcoal-extracted serum. There was no evidence of DNA fragmentation, consistent with the conclusion that the cells did not undergo apoptosis upon estrogen withdrawal. Hence, although cell growth was hormonally regulated, there was no evidence that the cells underwent apoptosis upon hormone withdrawal, even though the level of Bcl-2 expression declined during this period of time.

We conclude that the level of Bcl-2 present in cells after hormone withdrawal is probably sufficient to inhibit apoptosis. This hypothesis will need further testing, as alternative hypotheses exist that would explain the findings. Nevertheless, apoptosis did not appear to be induced in MCF-7 cells by estrogen withdrawal.

Subsequent tasks address the induction of apoptosis in breast cancer cells using an agent that selectively disrupts ER calcium homeostasis, thapsigargin.

Task 2, Adapt established calcium assays to breast cancer cell system:

2a. Conditions for optimal loading of breast cancer cells with Fura-2 will be determined.
2b. Measurements of Fura-2 fluorescence in cells adherent to Aclar plates will be established.
2c. Measurements of cytosolic calcium and intracellular stores will be made in cells induced to undergo PCD.
2d. Methods of measuring the ER calcium pool using mag-fura-2 will be established.
2e. Calcium measurements by FACS will be performed.

The original grant application proposed using the intracellular calcium indicator, Fura-2 AM to assess the role of calcium in apoptosis. Since then more direct methods have been developed for measuring calcium in the ER (endoplasmic reticulum). We have therefore used one of these methods, the method of ER-targeted cameleons, to measure ER calcium concentration. Cameleons are green fluorescent protein derivatives targeted for expression within a specific organelle for the purpose of measuring the calcium concentration within that organelle (23). The technique is based on measuring fluorescence emission ratios of two green fluorescent protein variants linked by a calmodulin-binding sequence (24,23) (**Figure 5**). The fluorescence resonance energy transfer (FRET) between the two fluorophores produces calcium-dependent changes in the emission ratio that is used to monitor calcium within the ER or cytoplasm of living cells. This approach has the advantage of a genetically encoded indicator that works without cofactors and that can be targeted to specific intracellular locations. The cameleon used in our studies comprises tandem fusions of a blue- or cyan-emitting GFP mutant, calmodulin, the calmodulin-binding peptide M13, and an enhanced green- or yellow-emitting GFP (23) (**Figure 5**). Binding of calcium makes calmodulin wrap around the M13 domain, increasing FRET between the flanking green fluorescent proteins. Two separate cameleons having relatively high and low calcium affinities, 4er and 3er respectively, will be employed in our studies. The experiments summarized here employed 3er.

MDA-MB-468 breast cancer cells were plated onto modified tissue culture dishes, which have a partially removed bottom and a coverslip attached over the removed portion. A pcDNA3 vector including the cDNA encoding for the ER targeted 3er cameleons (23) was used at 1 µg/ml in the transfection solutions and cells were transiently transfected using Lipofectamine. Transfected cells were examined by laser scanning confocal microscopy 48 to 96 hours after transfection, documenting that cells expressing 3er cameleon display a reticular pattern of fluorescence that does not overlap with mitochondria (the latter are red, identified with Mitotracker). These findings indicate that the cameleon has been targeted to the ER. Further evidence is currently being collected to prove that the cameleon expression is limited to the ER lumen.

To measure ER calcium concentration, cells were incubated in HEPES buffered saline, pH 7.4, at room temperature. Individual cells were viewed on an inverted fluorescence

microscope equipped with a PTI photoscan adaptor with illumination by a 50 W mercury lamp transmitted through neutral density filters (ND 2.0 - 3.0), a 440 ± 10 nm excitation filter (filters and dichroic mirrors from Omega Optical), and either a 40x or 100x objective. Excitation light was reflected by a dichroic mirror (460nm DCLP) and passed through an adjustable aperture centered on the cell being studied. The aperture was adjusted to minimize background light. A second dichroic mirror (505nm DCLP) separated the emitted light, which passed through additional emission filters, at 480 ± 15 nm for EYFP and 535 ± 125 nm for ECFP. The emitted light was measured by photomultiplier tubes and the spatially averaged signals were digitized and stored at ~3 Hz. Following aperture adjustment, background light was measured at both emission wavelengths in the absence of cells, and these intensities were subtracted from the experimental signal light intensities. Data analysis was performed with adjustment for time-dependent photobleaching.

A typical tracing is shown in **Figure 6**. Each tracing plots the fluorescence emission ratio F535/F480 over time, reflecting the ratio of calcium-bound versus calcium-free cameleon in the ER. A series of parallel microcapillaries, fixed to an arm that is mounted in a micromanipulator, was used to make local solution changes to individual fields of cells. The microperfusion solutions are shown as a bar across the top of each figure and were prepared in HEPES buffered saline, pH 7.40: 1 μM ionomycin with 5 mM CaCl2, 1 μM ionomycin with 5 mM EGTA, and 100 nM thapsigargin. In MDA-MB-468 neo cells, addition of the ER calcium-ATPase inhibitor thapsigargin produced a gradual fall in ER emission ratio, indicating a decrease in ER calcium concentration (**Figure 6**). Converting the microperfusion solution to EGTA/ionomycin induced a marked decrease in emission ratio, corresponding to a state of minimal ER calcium content, whereas converting the microperfusion solution to CaCl2/ionomycin produced a marked increase in emission ratio, corresponding to a state of maximal ER calcium content. Based on these minimum and maximum values, together with in vitro calibration of emission ratio according to calcium concentration, the ER calcium concentration will be determined, as described elsewhere (23).

The technique of using ER-targeted cameleons to measure ER calcium content will be applied in ongoing studies to assess the effect of various apoptosis inducing signals on the ER calcium pool, thereby testing the role of ER calcium release in this process.

Task 3, Determine effect of thapsigargin on growth and viability of breast cancer cells:

3a. Measure effects of thapsigargin treatment on growth and viability of breast cancer cells over broad dose-response range. To determine the effect of the endoplasmic reticulum (ER) calcium pump inhibitor, thapsigargin (TG), on cell growth and viability in breast cancer cells, MCF-7 and MDA-MB-468 cells were treated with a range of concentrations of TG, known from previous studies to inhibit calcium uptake by the ER. Methods for use of TG have been described previously (14). We found that 100 nM was sufficient to inhibit cell proliferation. In both cell lines, treatment with 100 nM TG slowed cell growth and

15

induced loss of adherence properties. In MDA-MB-468 cells, treatment with 100 nM TG caused cell death, measured by increased incorporation of trypan blue dye, whereas TG treatment did not appear to induce cell death in MCF-7 cells.

Based on these initial observations, we proceeded directly to the next planned experiments, designed to measure morphological and biochemical parameters to determine whether TG-induced cell death was due to induction of apoptosis. Both MCF-7 and MDA-MB-468 cells were treated with TG, an ER calcium pump inhibitor that has been shown previously to induce apoptosis in lymphoma cells and prostate cancer cells (12,25). Nuclear chromatin condensation, a hallmark of apoptosis, was readily detected by fluorescence microscopy in TG-treated MDA-MB-468 cells, but was not detected in TG-treated MCF-7 cells (26). In contrast to MDA-MB-468 cells, MCF-7 cells were resistant to TG-induced apoptosis, whether or not they were cultured in charcoal extracted serum to remove endogenous estrogen. Thus, culturing MCF-7 cells under estrogen-free conditions did not increase their susceptibility to TG-induced apoptosis, indicating that the decrease in Bcl-2 level associated with estrogen deprivation is insufficient to increase the susceptibility of MCF-7 cells to apoptosis induction by TG.

3b. Measure morphological and biochemical parameters to determine whether thapsigargin-induced loss of viability is due to induction of apoptotic cell death. Recent findings indicate that apoptosis in general is mediated by proteases related to interleukin 1-ß converting enzyme. These proteases, known as caspases, compose a family of cysteine proteases that characteristically cleave proteins at aspartic acid residues (27,28). Cleavage of selected target proteins by caspase-3 and related is responsible for the stereotypic morphological changes characteristic of apoptosis (29). We therefore employed two strategies to determine whether or not TG-induced apoptosis was mediated by caspase-like proteases. In the first strategy, MDA-MB-468 cells were stably transfected with a cDNA encoding p35, a baculovirus inhibitor of ICE-like proteases. Methods were described in detail previously (26). Although p35 protein was not detected in lysates of stably transfected cells by Western blotting (not shown), p35 mRNA was readily detected by RT-PCR. Control, vector only, transfectants and p35 transfectants were examined before and after TG treatment to detect morphological changes typical of apoptosis (Figure 5 in ref. 26, reprint in Appendix). The proportion of apoptotic cells was quantified by examining ethidium bromide/acridine orange stained cells under fluorescence microscopy, by previously described methods (22). The results indicate that p35 inhibits TG-induced apoptosis.

In a second approach at testing the importance of caspase-like proteases in TG-induced apoptosis, cells were treated with TG in the presence or absence of the peptide fluoromethylketone inhibitor Z-VAD-fmk. The tripeptide sequence in Z-VAD-fmk corresponds to the P1 to P3 residues of the pro-IL-1ß cleavage site (Tyr4ValAlaAsp1Gly), where caspase-1 cleaves between the Asp and Gly residue (30). Deletion of the Tyr residue would be expected to broaden the inhibitory spectrum to include not only caspase-1, but

other proteases closely related to caspase-1. An effective treatment regimen was empirically derived in which cells were treated with 200 μM doses of Z-VAD-fmk added 1 h prior to TG, and every 12 h thereafter over a period of 48 h. In addition to Z-VAD-fmk, Z-FA-fmk, a cathepsin inhibitor, was employed as a negative control. Apoptosis induction by TG, measured by fluorescence microscopy, was inhibited by Z-VAD-fmk, but not the control inhibitor, Z-FA-fmk (Figure 6 in ref. 26, reprint in Appendix), thus confirming that ICE-like protease activity is necessary for mediating apoptosis in response to TG treatment.

These findings were published in Oncogene (26).

3c. Determine if cells adapt to growth in thapsigargin, and if cells so adapted become resistant to induction of PCD by hormonal manipulations. These experiments have not been attempted in breast cancer cell lines, although similar experiments have been conducted in lymphoma lines. The findings indicate that cells can be adapted to growth in increasing concentrations of thapsigargin. The mechanism appears to involve induction of thapsigargin-insensitive calcium pumps that restore calcium content to the ER (31).

3d. Measure other parameters of thapsigargin-induced endoplasmic calcium pool depletion, including transcriptional induction of grp78 and grp94 genes, alterations of protein processing, and capacitative calcium entry. Although the preceding findings indicate that TG induces apoptosis in breast cancer cells, we observed that the onset of cell death was much slower than in lymphoid cells. For example, we found that certain lymphoma cell lines undergo apoptosis within less than 12 h following addition of 100 nM TG (12). In contrast, only a modest increase in apoptotic cells was observed within the first 24 after adding 100 nM TG to MDA-MB-468 cells. To examine the mechanism underlying differences in the susceptibility of different cell types to apoptosis induction, we investigated the grp78/grp94 stress response to TG-induced ER calcium pool depletion in various cell types.

The ER is the major intracellular reservoir of calcium in non-muscle cells. The ER calcium pool is essential for a number of vital cellular functions which include protein processing within the ER, maintaining high translation rates of newly transcribed messages, preserving the structural integrity of the ER, and regulating cell proliferation and cell cycle progression. Under physiological conditions, the ER calcium pool is maintained by an associated calcium-ATPase that pumps calcium into the ER lumen from the cytoplasm. The ER calcium pool can be depleted by treating cells with the calcium ionophore A23187 or the selective ER calcium-ATPase inhibitor thapsigargin (TG). ER function is mediated, in part, by intraluminal calcium binding proteins which include the glucose regulated proteins (GRP's) GRP78 and GRP94. GRP78 and GRP94 are found constitutively within the ER, and transcription of the genes for these proteins is elevated in response to malfolded proteins, inhibition of glycosylation and ER calcium pool depletion. GRP78 is a highly conserved 78 kDa protein that shares 60% amino acid homology with the 70 kDa heat shock protein (HSP 70). GRP78 (also known as BiP) associates transiently with nascent

17

proteins as they traverse the ER and aids in their folding and transport. The binding of immature proteins by GRP78 requires ATP, and GRP78 has both ATP binding and ATPase activities. GRP94 is a 94 kDa glycoprotein that shares 50% amino acid homology with HSP90. GRP94 acts in concert with GRP78 to fold nascent proteins, and also exhibits ATPase activity.

In epithelial cells and fibroblasts, grp78 and grp94 are coordinately regulated through common calcium-responsive promoter elements that respond to ER calcium pool depletion. Thus, ER calcium pool depletion, induced by either A23187 or TG, signals an increase in grp78/grp94 transcription, producing a 5- to 20 fold elevation of grp78/grp94 mRNA levels. In these cells, the loss of ER calcium induced by TG or A23187 does not result in a loss of viability, unless the grp78/grp94 stress response is repressed by antisense, promoter competition or ribozyme techniques. Moreover, grp78/grp94 induction restores protein synthesis under conditions where intracellular calcium is depleted. This indicates that grp78/grp94 gene induction is a protective response mechanism by which cells accommodate to potentially lethal stress caused by the disruption of intracellular calcium homeostasis.

Based on this background information, we reasoned that the decreased susceptibility of breast cancer cells to apoptosis induction by TG, compared to lymphoma cells, might be secondary to differences in grp78/grp94 stress response induction. To test this hypothesis, we measured the level of grp78 mRNA following TG treatment in WEHI7.2 lymphoma cells and several breast cancer cell lines, Mm5MT, MCF-7, and MDA-MB-468. We found that TG induced calcium loss from the ER of WEHI7.2 cells does not induce grp78 transcription, even if cells are protected from undergoing apoptosis by overexpressing Bcl-2 (W.Hb12 is a subclone of WEHI7.2 cells stably transfected with cDNA encoding Bcl-2) (Figure 2 in ref. 22, reprint in Appendix). In contrast, grp78 transcription was strongly induced in each of the breast cancer cell lines (Figure 8 in ref. 22, reprint in Appendix).

In summary, these findings have two important implications. First, the grp78 stress response may be differentially regulated among different types of cells, with a much greater response observed in non-lymphoid cells than in lymphoid cells. Second, regulation of the grp78 stress response may be a major factor in deciding whether a cell lives or dies in response to disruption of intracellular calcium homeostasis. Indeed, the absence of a calcium-mediated grp78 stress response may be the basis for the marked susceptibility of certain lymphoma cells to TG-induced apoptosis, and the decreased susceptibility of breast cancer cells to TG-induced apoptosis.

These findings were published in The Journal of Biological Chemistry (22).

Task 4, Determine whether measures that interfere with endoplasmic reticulum calcium release inhibit PCD in breast cancer cells:

4a. Measure effects of intracellular calcium chelators and calcium antagonists on induction

18

of PCD. These experiments have not been attempted due to the fact that other experiments took precedence in terms of the time and funding available.

4b. Determine effect of elevated grp78 expression on PCD, including vector preparation, derivation of stably transfected cells, measurements of inducible grp78 expression, and assays to determine effect of induced expression on PCD.

The preceding findings indicate a direct correlation between the ability of cells to mount a strong grp78 stress response and resistance to apoptosis. To determine if this resistance is mediated through grp78 overexpression alone, we investigated the effect of enforced overexpression of grp78 on apoptosis induction in MDA-MB-468 breast cancer cells. The cDNA encoding hamster grp78 was cloned into the pSFFVneo expression vector. Cells were transfected with the pSFFVneo-grp78 expression vector. Stable transfectants were selected in G418 and multiple subclones were selected. The level of GRP78 protein in individual clones was measured by Western blotting on whole cell lysates. As shown in **Figure 7**, elevated expression was achieved in several clones. The effect of thapsigargin on the viability of these clones was compared to control transfectants. Thapsigargin treatment induced significant cell death in both the control transfectants and the GRP78 overexpressing clones. Thus, we conclude that elevated expression of GRP78 is not sufficient to protect cells from thapsigargin-induced apoptosis.

4c. Determine effect of elevated bcl-2 expression on PCD, including vector preparation, derivation of stably transfected cells, assays to confirm elevated levels of expression, and assays to determine effect of elevated expression on PCD.

To assess the effect of exogenous Bcl-2 in MDA-MB-468 cells, cells were stably transfected with an expression vector (pSFFVneo-Bcl-2) encoding human Bcl-2. Transfection was performed and individual clones were selected using G418. Western blotting analysis of whole cell lysates, using previously described methods (14), shows that Bcl-2 was significantly overexpressed in several clones (**Figure 8**). The effect of Bcl-2 on cell viability was measured following thapsigargin treatment. The findings indicate that Bcl-2 overexpression provided modest, but definite, protection against thapsgigargin-induced apoptosis (**Figure 8**).

Task 5, Determine how intracellular calcium fluxes contribute to PCD process:
5a. Conduct coimmunoprecitpitation assays to detect interaction between GRP78 and endonuclease, including preliminary work to establish endonuclease asssay.
5b. Conduct experiments to detect regulation of Grp78 endonuclease interaction by endoplasmic reticulum calcium pool.
5c. Develop Northern hybridization technique for assaying expression of c-fos and c-jun.
5d. Investigate regulation of c-fos and c-jun by endoplasmic reticulum-associated calcium fluxes.
5e. Investigate effect of antisense knockout of c-fos and c-jun on calcium-mediated PCD in breast cancer cells.

This work has not yet been initiated due to time constraints. It is often difficult to estimate exactly how long individual experiments will take to complete. Also, unexpected technical difficulties occasionally arise, even in the best of laboratories, that may delay the expected outcome of experiments. Furthermore, the very nature of research involves discovery of new and potentially important findings. Clarification and reproduction of such findings may take time that was not included within the time estimate of the original grant application. Research is not like a 30 second television commercial that provides an immediate answer and immediate gratification. Rather research requires continued thought and reassessment, and sometimes goes in unexpected directions that make precise estimates of time difficult. For these reasons, the first 4 tasks took somewhat longer than originally anticipated, and hence there was insufficient time to complete task 5.

CONCLUSIONS

In summary, the research described in this proposal should advance our understanding of the mechanism of PCD in breast cancer cells. Specific hypotheses will be tested with regard to the role of calcium, particularly mobilization of ER calcium, in the PCD pathway. It is anticipated that the knowledge gained from these studies should provide a background on which future studies can build toward the development of new therapeutic strategies for breast cancer based on triggering the PCD pathway.

REFERENCES

1. Steller, H. (1995) Science 267, 1445-1449
2. Thompson, C. B. (1995) Science 267, 1456-1462
3. Lefebvre, O., Wolf, C., Limacher, J.-N., Hutin, P., Wendling, c., LeMeur, M., Basset, P. and Rio, M.-C. (1992) J. Cell Biol. 119, 997-1002
4. Kyprianou, N., English, H. F., Davidson, N. E. and Isaacs, J. T. (1991) Cancer Res. 51, 162-166
5. Bardon, S., Vignon, F., Montcourrier, P. and Rochefort, H. (1987) Cancer Res 47, 1441-1448
6. Pagliacci, M. C., Tognellini, R., Grignani, F. and Nicoletti, I. (1991) Endocrinology 129, 2555-2562
7. Armstrong, D. K., Isaacs, J. T., Ottaviano, Y. L. and Davidson, N. E. (1992) Cancer Res. 52, 3418-3424
8. Bardon, S., Vignon, F., Montcourrier, P. and Rochefort, H. (1987) Cancer Res. 47, 1441-1448
9. Ellis, R. E., Yuan, J. and Horvitz, H. R. (1991) Annu. Rev. Cell Biol. 7, 663-698
10. Distelhorst, C. W. and Dubyak, G. (1998) Blood 91, 731-734
11. Connor, J., Sawzchuk, I. S., Benson, M. C. and al, e. (1988) Prostate 13, 119-130
12. Lam, M., Dubyak, G. and Distelhorst, C. W. (1993) Mol. Endocrinol. 7, 686-693
13. Jayaraman, T. and Marks, A. R. (1997) Mol. Cell Biol. 17, 3005-3012
14. Lam, M., Dubyak, G., Chen, L., Nuñez, G., Miesfeld, R. L. and Distelhorst, C. W. (1994)

Proc. Natl. Acad. Sci. USA 91, 6569-6573

15. Carafoli, E. (1987) Ann. Rev. Biochem. 56, 395-433
16. Little, E., Ramakrishnan, M., Roy, B., Gazit, G. and Lee, A. S. (1994) Crit. Rev. Eukaryotic Gene Express. 4, 1-18
17. Lam, M., Vimmerstedt, L. J., Schlatter, L. K., Hensold, J. O. and Distelhorst, C. W. (1992) Blood 79, 3285-3292
18. Ulatowski, L. M., Lam, M., Vanderburg, G., Stallcup, M. R. and Distelhorst, C. W. (1993) J. Biol. Chem. 268, 7482-7488
19. Baffy, G., Miyashita, T., Williamson, J. R. and Reed, J. C. (1993) J. Biol. Chem. 268, 6511-6519
20. Peitsch, M. C., Polzar, B., Stephan, H., Crompton, T., MacDonald, H. R., Mannherz, H. G. and Tschopp, J. (1993) EMBO J. 12, 371-377
21. He, H., Lam, M., McCormick, T. S. and Distelhorst, C. W. (1997) J. Cell Biol. 138, 1219-1228
22. McCormick, T. S., McColl, K. S. and Distelhorst, C. W. (1997) J. Biol. Chem. 272, 6087-6092
23. Miyawaki, A., Llopis, J., Heim, R., McCaffery, J. M., Adams, J. A., Ikura, M. and Tsien, R. Y. (1997) Nature 388, 882-887
24. Romoser, V. A., Hinkle, P. M. and Persechini, A. (1997) J. Biol. Chem. 272, 13270-13274
25. Furuya, Y., Lundmo, P., Short, A. D., Gill, D. L. and Isaacs, J. T. (1994) Cancer Res. 54, 6167-6175
26. Qi, X.-M., He, H., Zhong, H. and Distelhorst, C. W. (1997) Oncogene (in press),
27. Fraser, A. and Evan, G. (1996) Cell 85, 781-784
28. Henkart, P. A. (1996) Cell 4, 195-201
29. Martin, S. J. and Green, D. R. (1995) Cell 82, 349-352
30. Yuan, J., Shaham, S., Ledoux, S., Ellis, H. M. and Horvitz, H. R. (1993) Cell 75, 641-652
31. Waldron, R. T., Short, A. D. and Gill, D. L. (1995) J. Biol. Chem. 270, 11955-11961

APPENDICES

REPRINTS OF THE FOLLOWING PAPERS SUPPORTED BY THIS GRANT

Qi X-M, He H, Zhong H, Distelhorst CW. Baculovirus p35 and Z-VAD-fmk inhibit thapsigargin-induced apoptosis of breast cancer cells. Oncogene 15:1207-1212, 1997

McCormick TS, McColl KS, Distelhorst CW. Mouse lymphoma cells destined to undergo apoptosis in response to thapsigargin treatment fail to generate a calcium-mediated GRP78/GRP94 stress response. J Biol Chem 272:6087-6092, 1997.

BIBLIOGRAPHY (all publications and meeting abstracts)

<u>PUBLICATIONS</u>
Qi X-M, He H, Zhong H, Distelhorst CW. Baculovirus p35 and Z-VAD-fmk inhibit thapsigargin-

induced apoptosis of breast cancer cells. Oncogene 15:1207-1212, 1997

McCormick TS, McColl KS, Distelhorst CW. Mouse lymphoma cells destined to undergo apoptosis in response to thapsigargin treatment fail to generate a calcium-mediated GRP78/GRP94 stress response. J Biol Chem 272:6087-6092, 1997.

MEETING ABSTRACTS

Distelhorst, C.W., Qi, X-M., McColl, K.S., McCormick, T.S., Zhong, H., Lam, M. Differential sensitivity of breast cancer and lymphoma cells to thapsigargin-induced apoptosis is regulated by the GRP78/GRP94 stress response. Era of Hope Proceedings I: 335, 1997

List of personnel receiving pay from this effort

Distelhorst, Clark W.   Principal Investigator

Qi, Xiao-Mei,   Research Assistant

Figure Legends

Figure 1: Bcl-2 expression in MDA-MB-468 cells. A, Western blot comparing levels of Bcl-2 in MCF-7 and MDA-MB-468 cells. B, Western blot showing levels of Bcl-2 in MDA-MB-468 cells stably transfected with an expression vector encoding Bcl-2 or neo control vector. C, Western blot showing the increase in Bcl-2 level that occurs when MDA-MB-468 cells are allowed to remain in culture after they have become confluent.

Figure 2: Effect of estrogen on Bcl-2 expression in MCF-7 cells. A, cell growth in tissue culture medium supplemented with unextracted serum (Reg Med) or medium supplemented with charcoal extracted serum (Ext Med). B, Western blot comparing Bcl-2 levels in cells at various time points after cells were suspended in either Reg Med or Ext Med. C, Bcl-2 levels were compared by scanning densitometry of Western blots similar to that shown in panel B. Results represent the mean ± SE of multiple experiments.

Figure 3: Effect of estrogen restoration on Bcl-2 expression in cells cultured in regular medium versus extracted medium. 17ß-estradiol was added as described in the text to MCF-7 cells cultured in either regular medium or extracted medium (see Figure 2 for definition) and the fold induction of Bcl-2 level was measured by Western blotting. Results represent the mean ± SE or multiple experiments.

Figure 4: Effect of estrogen supplementation on cell proliferation for MCF-7 cells cultured in either regular medium (Reg) or medium supplemented with charcoal extracted serum (Ext). MCF-7 cells were cultured in either regular medium or medium

supplemented with charcoal extracted serum for the times shown in either the presence or absence of 17ß-estradiol. Cell numbers represent the mean ± SE of multiple experiments.
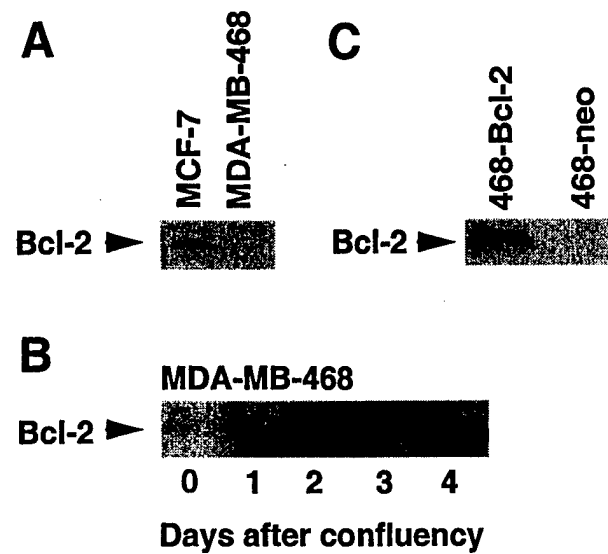
Figure 5: Schematic structure of cameleons. Two different fluorescent protein derivatives, ECFP and EYFP, are linked together by a calmodulin (CaM)/M13 sequence, as described by Miyawaki et al (22). The binding of calcium to calmodulin induces a conformational change which brings the two fluorescent proteins into spatial proximity, allowing fluorescence resonance energy transfer (FRET) between the two proteins. Hence, the emission ratio (F535/F480) reflects the ratio of calcium-bound to calcium-free cameleon in the endoplasmic reticulum.

Figure 6: Measurement of ER calcium concentration using ER-targeted cameleon 3er. The cameleon 3er was targeted to the ER of MDA-MB-468 cells in a transient transfection experiment. The emission intensities, F535 and F480, were measured simultaneously on a single cell basis. The ratio of emission intensities is shown as the uppermost tracing, while the dashed line represents the baseline emission ratio. Sequential additions of Hank's balanced salt solution (HBS), thapsigargin (TG), EGTA/iono (ionomycin), CaCl2/iono are shown.

Figure 7: Effect of grp78 overexpression on thapsigargin-induced cell death. Upper panel, MCF-7 cells were stably transfected with pSFFV-plasmid carrying hamster grp78 full length cDNA and single colonies were isolated. Whole cell lysates wee prepared for Western blotting with monoclonal antibodies toward GRP78. Lane 1, pSFFV-neo control; lanes 2-4, GRP78 overexpressing clones 7,8, and 11. Lower panel, GRP78 overexpressing MCF-7 cells and their controls were treated with 100 nM thapsigargin and viability was determined 12 and 72 hr after exposure with propidium iodide assay.

Figure 8: Effect of Bcl-2 overexpression on thapsigargin-induced apoptosis. Upper panel, MDA-MB-468 cells were stably transfected with pSFFV-neo vector carrying full length Bcl-2 cDNA or empty vector (pSFFV-neo) and single clones were isolated. Whole cell lysates were prepared for Western blot analysis with monoclonal antibody towards human Bcl-2. Lane 1, wild type (wt); lane 2, pSFFV-neo; lanes 3-5, Bcl-2 overexpressing clones Mb6, Mb9, Mb10.
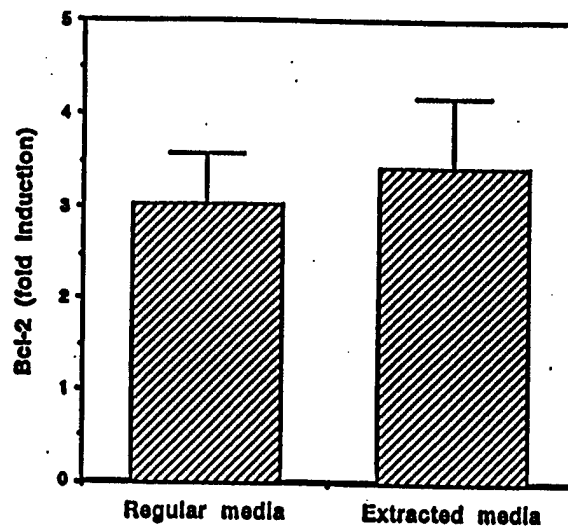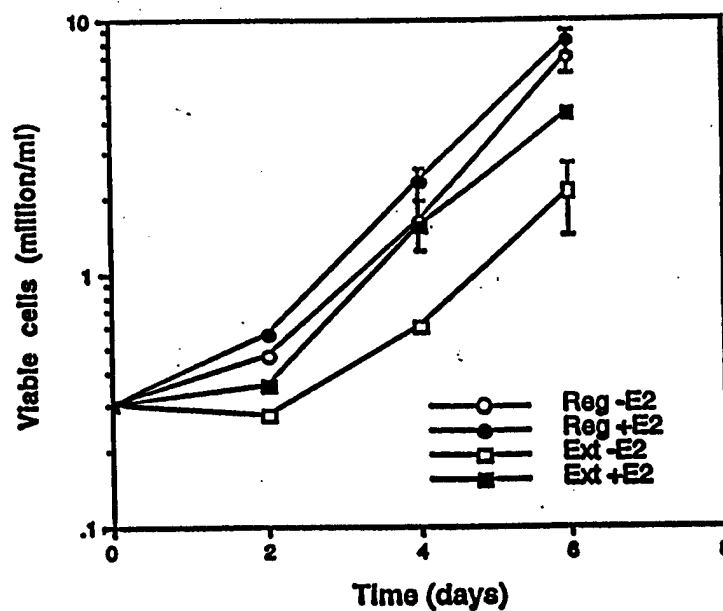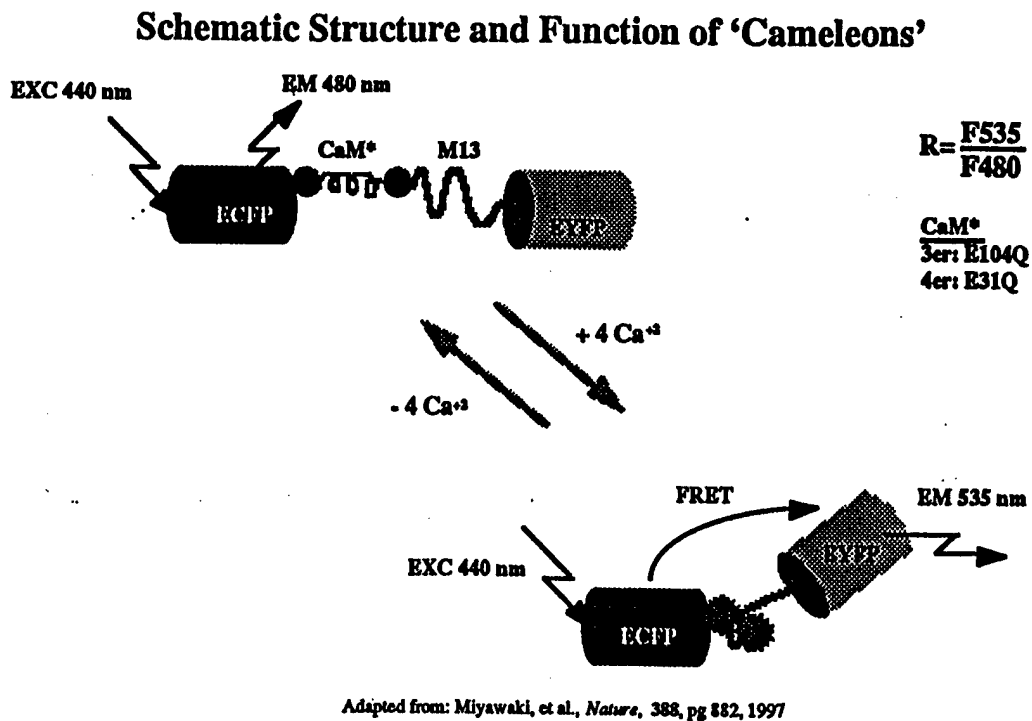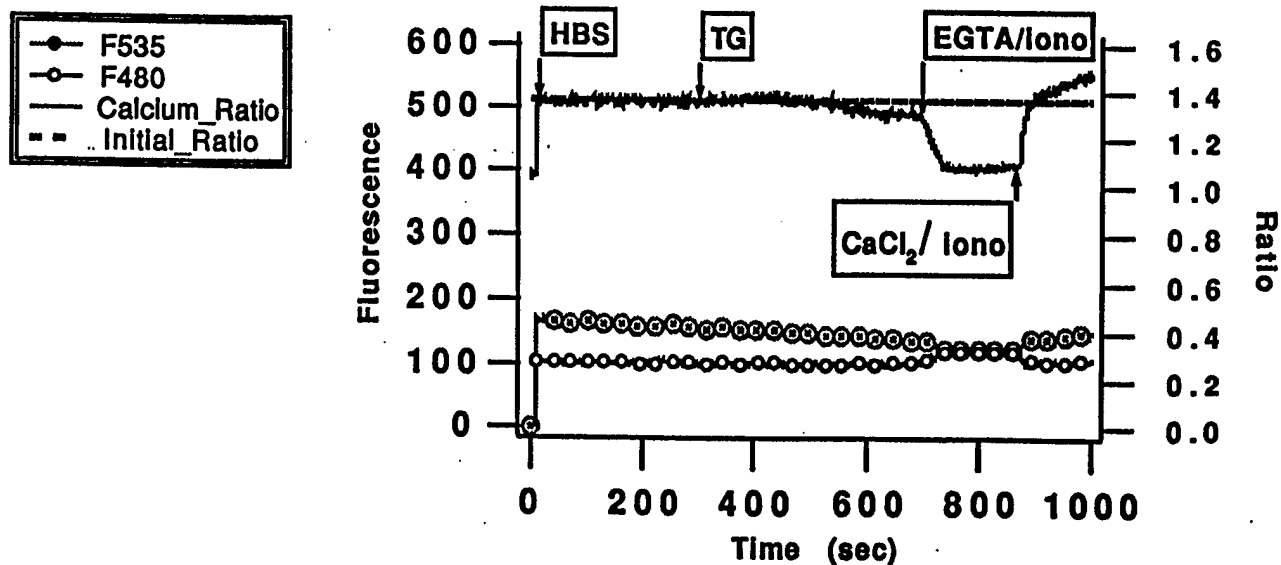
Fig. 1: Bcl-2 expression in MDA-MB-468 cells

A

MCF-7 MDA-MB-468

Bcl-2 ▶

C

468-Bcl-2 468-neo

Bcl-2 ▶

B

MDA-MB-468

Bcl-2 ▶

0 1 2 3 4

Days after confluency

Fig. 2: Effect of estrogen on Bcl-2 expression in MCF-7 cells.
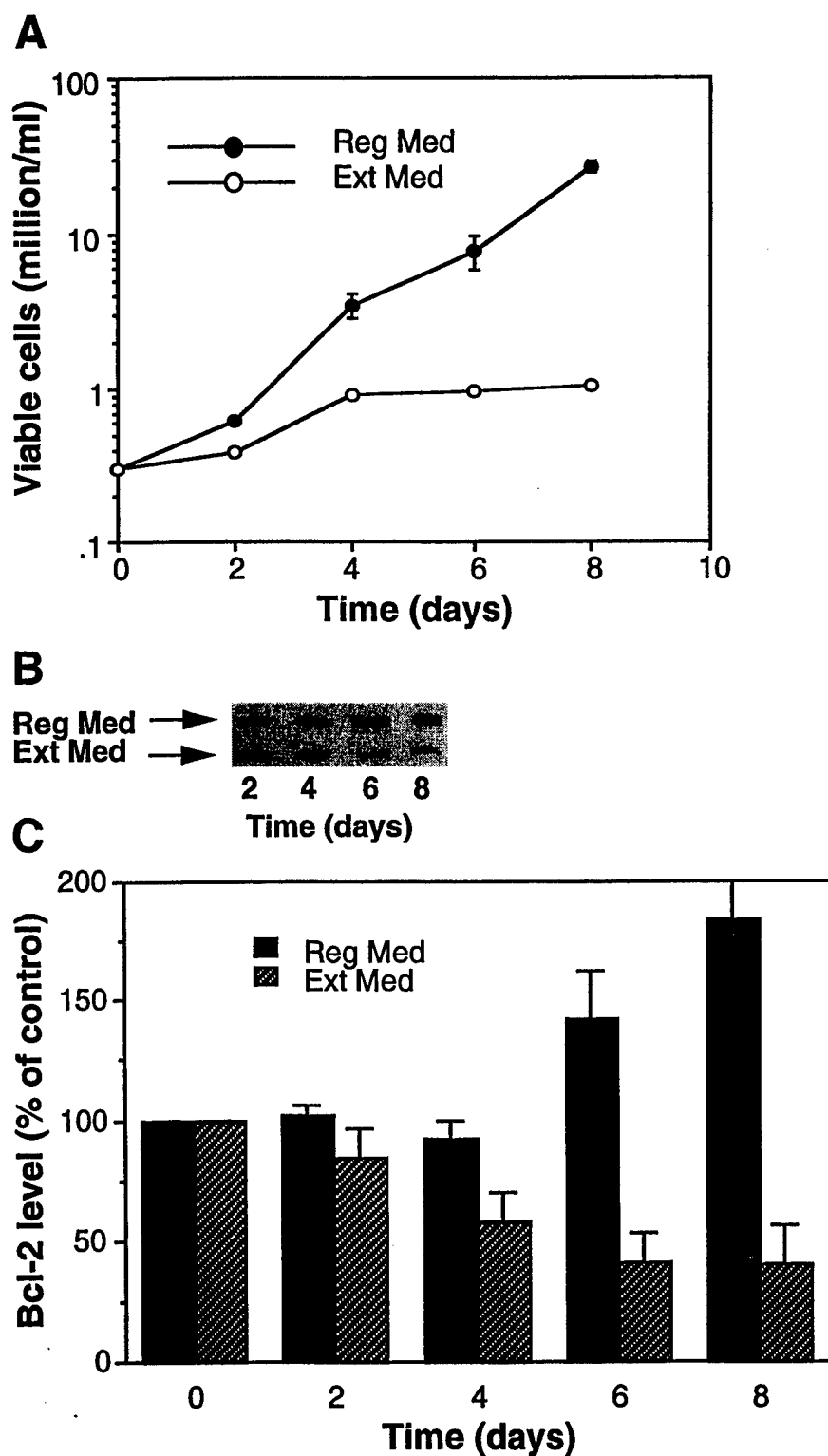
Figure 3: Effect of estrogen restoration on Bcl-2 expression in cells cultured in regular medium versus extracted medium.

Figure 4: Effect of estrogen supplementation on cell proliferation for MCF-7 cells cultured in either regular medium (Reg) or medium supplemented with charcoal extracted serum (Ext).

Figure 5

Schematic Structure and Function of 'Cameleons'

EXC 440 nm   EM 480 nm   CaM*   M13

ECFP   EYFP

$$R = \frac{F535}{F480}$$

CaM*
3er: E104Q
4er: E31Q

+ 4 Ca^{+2}

- 4 Ca^{+2}

FRET   EM 535 nm

EXC 440 nm   ECFP   EYFP

Adapted from: Miyawaki, et al., *Nature*, 388, pg 882, 1997

Figure 6 : Measurement of ER calcium concentration using ER-targeted cameleon 3er.

Legend:
- ● F535
- ○ F480
- — Calcium_Ratio
- ▪ ▪ Initial_Ratio

HBS   TG   EGTA/Iono   CaCl$_2$/ Iono

Fluorescence: 0, 100, 200, 300, 400, 500, 600
Ratio: 0.0, 0.2, 0.4, 0.6, 0.8, 1.0, 1.2, 1.4, 1.6
Time (sec): 0, 200, 400, 600, 800, 1000

1 2 3 4
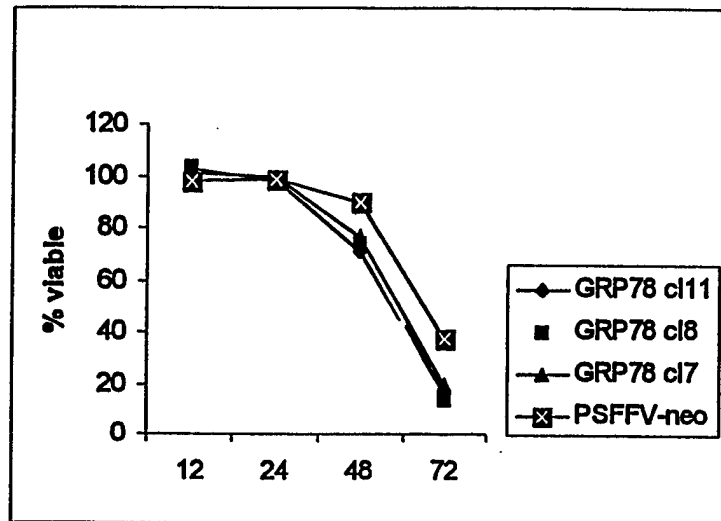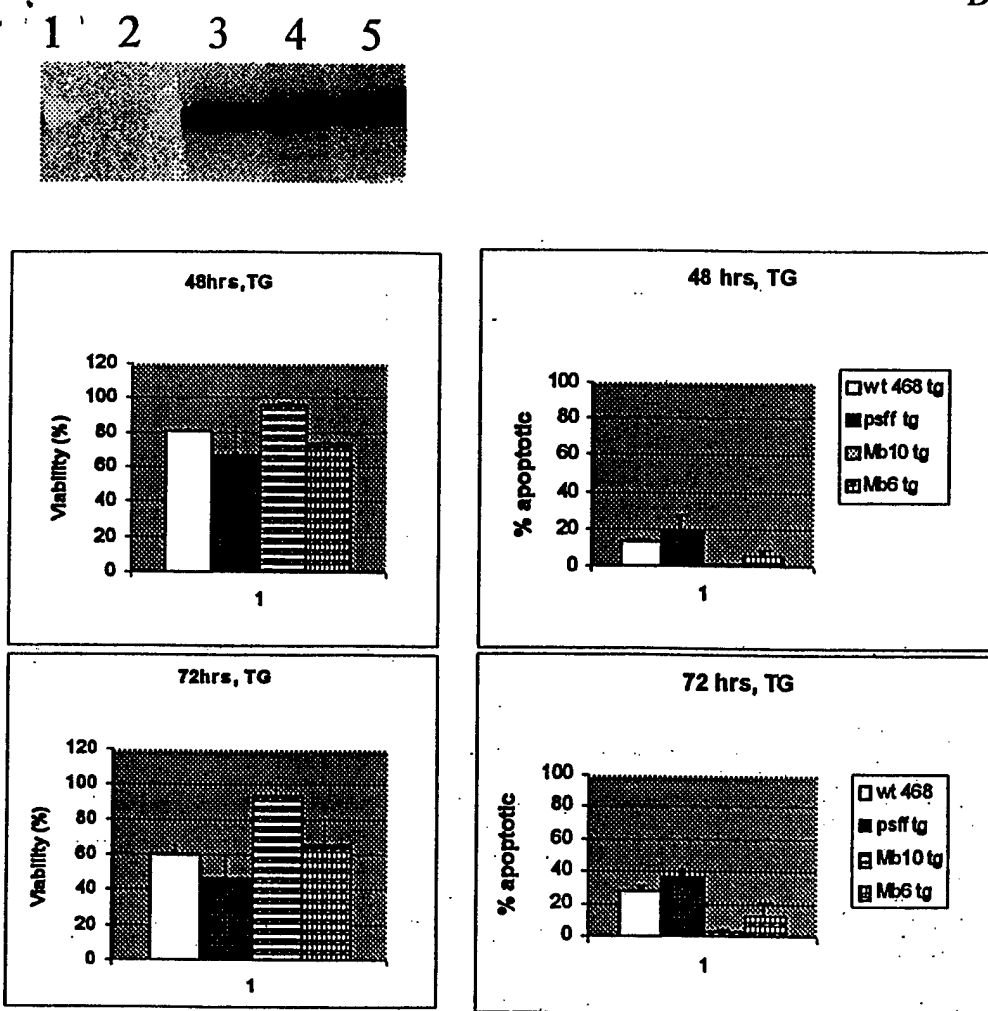
Figure 7

Figure 8

Mouse Lymphoma Cells Destined to Undergo Apoptosis in Response to Thapsigargin Treatment Fail to Generate a Calcium-mediated *grp78/grp94* Stress Response*

Thomas S. McCormick‡§, Karen S. McColl‡, and Clark W. Distelhorst¶

From the Department of Medicine, Case Western Reserve University School of Medicine and the Ireland Cancer Center, University Hospitals of Cleveland, Cleveland, Ohio 44106

grp78/grp94 induction is critical for maintaining the viability of epithelial cells and fibroblasts following treatment with thapsigargin (TG), an inhibitor of Ca^{2+} uptake into the endoplasmic reticulum. In contrast to these cell types, WEHI7.2 mouse lymphoma cells undergo apoptosis when treated with TG, prompting us to examine the *grp78/grp94* stress response in WEHI7.2 cells. TG treatment failed to induce *grp78/grp94* transcription in WEHI7.2 cells, measured by Northern hybridization and nuclear run-on assays, even if the cells were protected from apoptosis by overexpressing *bcl-2*. However, *grp78/grp94* transcription was induced by the glycosylation inhibitor tunicamycin, suggesting that there are at least two *grp78/grp94* signaling pathways, one in response to TG-induced endoplasmic reticulum Ca^{2+} pool depletion, which is inoperable in WEHI7.2 cells, and one in response to glycosylation inhibition, which is operable in WEHI7.2 cells. Studies of additional lymphoid lines, as well as several nonlymphoid lines, suggested a correlation between *grp78/grp94* induction and resistance to apoptosis following TG treatment. In conclusion, the vulnerability of TG-treated WEHI7.2 cells to apoptosis may be due to failure to signal a *grp78/grp94* stress response.

The endoplasmic reticulum (ER)[1] is the major intracellular reservoir of Ca^{2+} in nonmuscle cells (1). The ER Ca^{2+} pool is essential for a number of vital cellular functions, which include protein processing within the ER (2, 3), maintaining high translation rates of newly transcribed messages (4), preserving the structural integrity of the ER (5, 6), and regulating cell proliferation and cell cycle progression (7). Under physiological conditions, the ER Ca^{2+} pool is maintained by an associated Ca^{2+}-ATPase that pumps Ca^{2+} into the ER lumen from the cytoplasm (8). The ER Ca^{2+} pool can be depleted by treating cells with the Ca^{2+} ionophore A23187 or the selective ER Ca^{2+}-ATPase inhibitor thapsigargin (TG) (9).

ER function is mediated, in part, by intraluminal Ca^{2+}-binding proteins, which include the glucose-regulated proteins GRP78 and GRP94 (5, 10, 11). GRP78 and GRP94 are found constitutively within the ER, and transcription of the genes for these proteins is elevated in response to malfolded proteins, inhibition of glycosylation, and ER Ca^{2+} pool depletion (12–14). GRP78 is a highly conserved 78-kDa protein that shares 60% amino acid homology with the 70-kDa heat shock protein (HSP70). GRP78 (also known as BiP) associates transiently with nascent proteins as they traverse the ER and aids in their folding and transport (15–20). The binding of immature proteins by GRP78 requires ATP, and GRP78 has both ATP binding and ATPase activities (21). GRP94 is a 94-kDa glycoprotein that shares 50% amino acid homology with HSP90 (11, 22). GRP94 acts in concert with GRP78 to fold nascent proteins and also exhibits ATPase activity (22–24).

In epithelial cells and fibroblasts, *grp78* and *grp94* are coordinately regulated through common Ca^{2+}-responsive promoter elements that respond to ER Ca^{2+} pool depletion (10, 25). Thus, ER Ca^{2+} pool depletion, induced by either A23187 or TG, signals an increase in *grp78/grp94* transcription, producing a 5–20-fold elevation of *grp78/grp94* mRNA levels (25). In these cells, the loss of ER Ca^{2+} induced by TG or A23187 does not result in a loss of viability, unless the *grp78/grp94* stress response is repressed by antisense, promoter competition, or ribozyme techniques (26–28). Moreover, *grp78/grp94* induction restores protein synthesis under conditions where intracellular Ca^{2+} is depleted (29). This indicates that *grp78/grp94* gene induction is a protective response mechanism by which cells accommodate to potentially lethal stress caused by the disruption of intracellular Ca^{2+} homeostasis.

In contrast to epithelial cells and fibroblasts, we have found that WEHI7.2 mouse lymphoma cells undergo apoptosis in response to TG-induced ER Ca^{2+} loss, unless protected by overexpression of the anti-apoptotic oncogene *bcl-2* (30). Given this observation, we chose to examine the *grp78/grp94* stress response in WEHI7.2 mouse lymphoma cells. We report for the first time that TG-induced Ca^{2+} loss from the ER of WEHI7.2 cells does not induce *grp78/grp94* transcription, even if cells are protected from undergoing apoptosis by *bcl-2*. Interestingly, treatment with tunicamycin (TN), an inhibitor of N-linked glycosylation, does induce *grp78/grp94* transcription, suggesting that ER Ca^{2+} pool depletion and accumulation of underglycosylated proteins signal an increase in *grp78/grp94* transcription through independent pathways, the former pathway being inoperative in WEHI7.2 cells. Moreover, in three breast cancer cell lines and two additional lymphoma lines, the induction of *grp78* correlated with resistance to TG-induced apoptosis. These findings suggest that inherent differences in the susceptibility of cells to apoptosis induction by TG can be determined, at least in part, by the cell's capacity to mount a *grp78/grp94* stress response.

[1] The abbreviations used are: ER, endoplasmic reticulum; TG, thapsigargin; TN, tunicamycin.

EXPERIMENTAL PROCEDURES

Materials—TG was purchased from LC Laboratories, serum from Hyclone Laboratories, and TN from Calbiochem. L-Glutamine, antibiotics, and nonessential amino acids were from Life Technologies, Inc. All other chemicals, unless noted otherwise, were obtained from Sigma.

Cell Culture and Treatment Conditions—The WEHI7.2 mouse lymphoma cell line, which does not express detectable levels of Bcl-2, was stably transfected with a cDNA encoding full-length human *bcl-2*, yielding the W.Hb12, W.Hb13, and W.Hb15 clones employed in the present study (30). Two additional Bcl-2-negative mouse lymphoma cell lines, S49.1 and W7.MG1, have been described previously (31). Lymphoma lines were maintained in Dulbecco's modified Eagle's medium (Bio-Whittaker, Inc.) supplemented with 10% (v/v) heat-inactivated horse serum, 2 mM glutamine, 50 units/ml penicillin, 50 μg/ml streptomycin, and 0.4 mM nonessential amino acids at 37 °C in a 7% CO_2 atmosphere. Cells were maintained at a density of 0.2–1.5 $\times$ 10^6/ml by dilution into fresh culture medium three times weekly. Mm5MT mouse mammary cells (obtained from American Type Culture Collection) were maintained in the same culture medium as lymphoma lines, supplemented with 10 μg/ml bovine insulin. MDA-MB-468 human breast cancer cells (from M. Lippman, Georgetown University) were cultured in improved minimal essential medium (Biofluids, Inc.) supplemented with 10% (v/v) heat-inactivated fetal bovine serum, 2 mM glutamine, 50 units/ml penicillin, 50 μg/ml streptomycin, and 0.4 mM nonessential amino acids at 37 °C in a 7% CO_2 atmosphere. MCF-7 human breast cancer cells (from S. Gerson, Case Western Reserve University) were cultured in RPMI 1640 medium (Cancer Center Tissue Culture Core Facility) supplemented with 10% (v/v) heat-inactivated fetal bovine serum, 25 μg/ml bovine insulin, 2 mM glutamine, 50 units/ml penicillin, 50 μg/ml streptomycin, and 0.4 mM nonessential amino acids at 37 °C in a 7% CO_2 atmosphere.

A 1 mg/ml stock of TG was made in dimethyl sulfoxide and stored in aliquots at −20 °C. A working stock was prepared by diluting TG in fresh culture medium to a final concentration of 1 μM. TG was then added to the cell cultures to achieve the desired final concentrations as noted below. Untreated cultures received the same volumes of dimethyl sulfoxide without TG. A 5 mg/ml stock of TN was prepared in dimethyl sulfoxide and stored at room temperature. TN was added to the cell cultures to a final concentration of 0.75 μM. Untreated cultures received the same volumes of dimethyl sulfoxide without TN. Cell viability was assessed by counting cells on a hemocytometer after suspension in trypan blue dye.

Western Blotting—Levels of Bcl-2 protein were measured by Western blotting as described previously (30), using a human monoclonal anti-Bcl-2 antibody (Pharmingen). GRP78 and GRP94 levels were measured by Western blotting as described previously (31), using a monoclonal antibody to GRP78 (provided by D. Bole, University of Michigan) (15) or a rabbit polyclonal antibody to GRP94 (α-HS3) that immunocross-reacts with GRP78 (provided by M. Green, St. Louis University) (32).

Northern Blot Analysis—Total RNA was isolated from cells using Trizol (Life Technologies, Inc.). 10 or 20 μg of RNA were separated according to size on a 1.2% agarose gel with 2.2 M formaldehyde (final concentration). After separation, the RNA was transferred to a Zeta-Probe membrane (Bio-Rad) for 3 h (Schleicher & Schuell Turboblotter). Plasmids encoding cDNA for *grp78* (p3C5 from A. Lee, University of Southern California), *grp94* (pcDER99-2 from M. Green), and CHO-B (from M. Wilson, Scripps Clinic and Research Foundation) were used as the templates for polymerase chain reaction amplification of the specific cDNA inserts of interest. Probes were prepared by labeling with [α-^{32}P]dCTP via random priming of the polymerase chain reaction-amplified insert (Stratagene Prime-it kit). Use of polymerase chain reaction-amplified fragments as the template for random-primed probes eliminated a cross-reacting second band generated by the plasmid vector. Zeta-Probe membranes were prehybridized for 30 min at 65 °C in a buffer containing 1 mM EDTA, 0.5 M NaH$_2$PO$_4$, pH 7.2, and 7% SDS. The membranes were incubated overnight at 65 °C in fresh hybridization buffer containing one of the labeled probes. After hybridization, the membranes were washed twice at 65 °C for 15 min each in a buffer containing 1 mM EDTA, 40 mM Na$_2$HPO$_4$, pH 7.2, and 5% SDS. After the first two washes, the membrane was monitored for background. If needed, a final wash using 1 mM EDTA, 40 mM Na$_2$HPO4, pH 7.2, and 1% SDS was done at 65 °C for 15 min. The membranes were exposed to Kodak XAR-5 x-ray film at −80 °C. Blots were probed with radiolabeled DNA complementary to *grp78* or *grp94* mRNA, exposed to film, and then subsequently probed with radiolabeled DNA complementary to CHO-B mRNA. Blots were not stripped between hybridizations and were stored moist at 4 °C. Pre- and post-treatment levels of the

mRNA for *grp78* and *grp94* were quantitated by densitometry using a SciScan 5000 (U. S. Biochemical Corp.) with Oberlin Scientific Bio-analysis software and were normalized according to the constitutive level of CHO-B mRNA. Statistical differences were derived using a paired *t* test of the mean values.

Nuclear Run-off—Nuclear run-off assays were performed using modifications of previously published techniques (33–35). After culture with the appropriate agent, WEHI7.2 and W.Hb12 cells (5 $\times$ 10^7 cells/reaction) were centrifuged at 500 $\times$ *g* for 5 min at 4 °C and washed twice in ice-cold phosphate-buffered saline. Following the second wash, the cells were resuspended in cell lysis buffer (10 mM Tris-Cl, pH 7.4, 3 mM CaCl$_2$, and 2 mM MgCl$_2$) in a total volume of 40 ml. The cells were centrifuged at 1000 $\times$ *g* for 5 min, resuspended in 1 ml of cell lysis buffer, and added to 1 ml of Nonidet P-40 lysis buffer (10 mM Tris-Cl, pH 7.4, 10 mM NaCl, 3 mM MgCl$_2$, and 0.5% Nonidet P-40). After resuspension, the cells were homogenized using a Dounce homogenizer fitted with a B pestle. Phase-contrast microscopic examination of the cell suspension was used to determine that the cells were free of membrane components. Nuclei were collected by centrifugation of the homogenized cells at 500 $\times$ *g* for 5 min. The nuclear pellet was resuspended in 100 μl of glycerol storage buffer (50 mM Tris-Cl, pH 8.3, 40% (v/v) glycerol, 5 mM MgCl$_2$, and 0.1 mM EDTA), frozen in liquid nitrogen, and stored at −80 °C. Run-off transcription was initiated by resuspending the frozen nuclei in 100 μl of a reaction mixture containing 10 mM Tris-Cl, pH 8.0, 5 mM MgCl$_2$, 0.3 M KCl, 1 mM dithiothreitol, 40 units/ml RNasin, 1 mM ATP, 1 mM GTP, 1 mM CTP, and 25 μl of [α-^{32}P]UTP (3000 Ci/mmol) at 30 °C for 30 min. The DNA was then digested by adding 1 μl of 20,000 units/ml RNase-free DNase. Yeast tRNA (5 μl of 10 mg/ml) was added after the DNA digestion. Newly transcribed RNA was purified by adding 500 μl of a guanidinium thiocyanate solution (4 M guanidinium thiocyanate, 25 mM sodium citrate, pH 7.0, 0.5% *N*-lauroylsarcosine, and 0.1 M β-mercaptoethanol). The ^{32}P-labeled RNA was isolated by phenol/chloroform extraction followed by precipitation with sodium acetate (70 μl of 2.0 M) and 1 volume of isopropyl alcohol at −20 °C for 1 h in a microcentrifuge tube. The RNA was pelleted by microcentrifugation at 12,000 rpm for 30 min at 4 °C. The pellet was washed once with 70% ethanol and repelleted at 12,000 rpm for 5 min at 4 °C. The ^{32}P-labeled RNA was denatured by heating at 60 °C in 6 $\times$ SSPE, 1 $\times$ Denhardt's solution, 0.5% (w/v) SDS, and 50% (v/v) formamide. Total cpm of ^{32}P were equilibrated and hybridized to slot-blotted cDNAs for 60 h at 42 °C in 6 $\times$ SSPE and 1 $\times$ Denhardt's solution (0.5% SDS, 50 μg/ml denatured salmon sperm DNA, and 50% formamide). Following hybridization, the filters were washed in 2 $\times$ SSPE and 0.1% SDS at 42 °C for 30 min and then rewashed once for 20 min in 0.2 $\times$ SSPE and 0.1% SDS at 56 °C. After washing, the filters were exposed to Kodak XAR-5 film.

Slot Blot—65 μg of plasmid DNA (for *grp78*, *grp94*, pBR322, and pCHO-B) were linearized with the appropriate restriction enzyme in a final volume of 300 μl. The DNA was denatured by addition of 33 μl of 1 N NaOH and boiled for 10 min. The linearized DNA was neutralized by addition of 6 $\times$ SSC to a final volume of 1.5 ml and placed on ice for 5 min. 125 μl of DNA were added per slot (final concentration of 5 μg/slot) and drawn onto the filter by vacuum. After adding the plasmid DNA, the filter was washed once with 6 $\times$ SSC and once with 2 $\times$ SSC and baked for 30 min at 80 °C.

RESULTS

The susceptibility to cell death following TG treatment was investigated in WEHI7.2 cells, which do not express Bcl-2, and in stable transfectants that express either a low level of Bcl-2 (W.Hb13) or a high level of Bcl-2 (W.Hb12 and W.Hb15) (Fig. 1A). Consistent with earlier findings (30), WEHI7.2 cells rapidly lost viability following treatment with 100 nM TG, whereas a derivative expressing a low level of Bcl-2 (W.Hb13) was killed more slowly, and derivatives expressing a high level of Bcl-2 (W.Hb12 and W.Hb15) were resistant to TG-induced cell death (Fig. 1B).

Steady-state levels of *grp78* mRNA following TG treatment were assessed by Northern blot analysis (Fig. 2). The constitutively expressed marker CHO-B was used to control for minor loading differences as described under "Experimental Procedures." As shown by the Northern blot in Fig. 2A, the *grp78* mRNA level did not appear to increase following treatment of WEHI7.2 cells with 100 nM TG. In multiple experiments, the ratio of post-treatment to pretreatment levels was quantitated

A

Bcl2 →

B
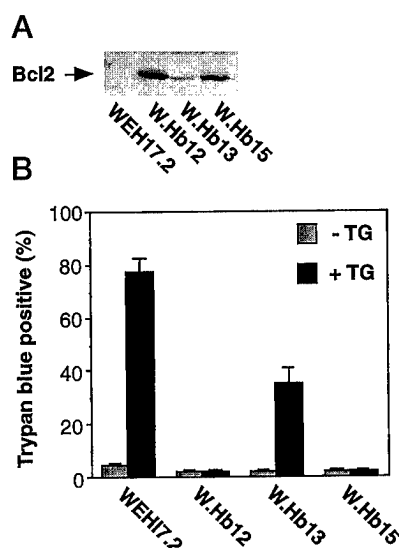
FIG. 1. **Effect of Bcl-2 on WEHI7.2 viability after TG treatment.** *A*, using an antibody specific for human Bcl-2, the levels of Bcl-2 protein expressed by WEHI7.2 cells and stable transfectants are shown by Western blot analysis. *B*, exponentially growing cells were diluted to a concentration of 0.3×10^6/ml with fresh culture medium 24 h before adding 100 nM TG at the zero time point. The percentage of trypan blue-positive cells was measured 24 h after TG addition. *Error bars* represent the mean of duplicate determinations in multiple experiments.

A

WEHI7.2

grp78 →

CHO B →

0 1 3 5 7 16 24
Time (h)

B

W.Hb12

grp78 →

CHO B →

0 1 3 5 7 16 24
Time (h)
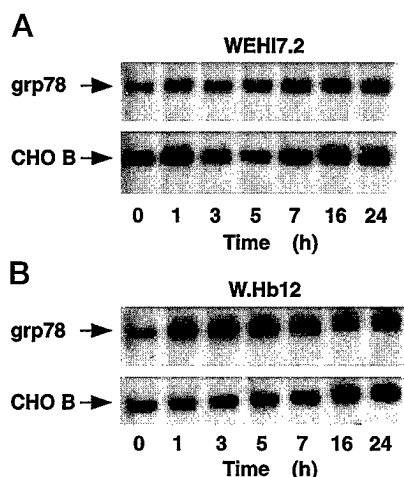
FIG. 2. **Effect of TG treatment on *grp78* mRNA levels in WEHI7.2 and W.Hb12 cells.** Exponentially growing cells were diluted to a concentration of 1×10^6/ml with fresh culture medium before adding 100 nM TG. RNA was isolated at the indicated times following TG addition and analyzed by Northern hybridization using radiolabeled *grp78* and CHO-B cDNA probes. Representative blots for WEHI7.2 cells (*A*) and W.Hb12 cells (*B*) are shown.

at each time point by densitometry with normalization to the CHO-B standard. The maximum ratio was 1.7 ± 0.2, which did not represent a reproducible elevation above pretreatment levels ($p \geq 0.05$). The failure of TG treatment to induce an elevation of the *grp78* mRNA level was confirmed at several other concentrations of TG (10, 50, and 300 nM) (data not shown).

To determine whether or not the failure of TG treatment to increase *grp78* mRNA levels in WEHI7.2 cells was secondary to early changes accompanying cell death, we examined the *grp78* stress response in W.Hb12 cells, which are protected from apoptosis by *bcl-2*. As shown by the Northern blot in Fig. *2B*, the *grp78* mRNA level did not appear to increase following treatment of W.Hb12 cells with 100 nM TG. In multiple experiments, the maximum post-treatment to pretreatment *grp78*

A

W.Hb13

grp78 →

CHO B →

0 1 3 5 7 16 24
Time (h)

B

W.Hb15

grp78 →

CHO B →

0 1 3 5 7 16 24
Time (h)
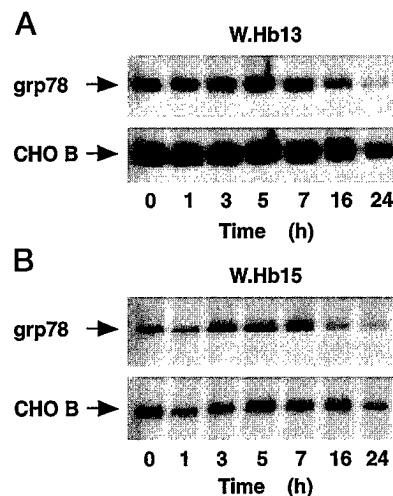
FIG. 3. **Effect of TG treatment on *grp78* mRNA levels in W.Hb13 and W.Hb15 cells.** Exponentially growing cells were diluted to a concentration of 1×10^6/ml with fresh culture medium before adding 100 nM TG. RNA was isolated at the indicated times following TG addition and analyzed by Northern hybridization using radiolabeled *grp78* and CHO-B cDNA probes. Representative blots for W.Hb13 cells (*A*) and W.Hb15 cells (*B*) are shown.

mRNA ratio was 2.1 ± 0.4, which did not represent a significant elevation above pretreatment levels ($p \geq 0.05$). Northern blot analysis of two other Bcl-2-expressing clones, W.Hb13 and W.Hb15, confirmed that *grp78* mRNA levels did not increase following treatment with 100 nM TG (Fig. 3, *A* and *B*). Note that in Fig. 3, *grp78* mRNA levels actually decreased relative to CHO-B levels at 16 and 24 h after TG addition. This observation was variable among experiments, including those with WEHI7.2 and W.Hb12 cells. Note that we have previously shown, in WEHI7.2 cells and derivatives expressing Bcl-2, that TG treatment inhibits the ER Ca^{2+}-ATPase, producing cytosolic Ca^{2+} elevation and ER Ca^{2+} pool depletion (30, 36). Hence, the failure to significantly elevate *grp78/grp94* transcription following TG treatment is not due to a failure of TG to disrupt Ca^{2+} homeostasis.

Levels of GRP78 and GRP94 proteins, assessed by Western blotting, were the same in untreated WEHI7.2 and W.Hb12 cells, indicating that *bcl-2* does not affect basal levels of GRP78/GRP94 expression at the protein level (Fig. 4, *A* and *B*). Furthermore, levels of GRP78 protein did not increase following TG treatment in either WEHI7.2 or W.Hb12 cells (Fig. 4*C*).

Both WEHI7.2 and W.Hb12 cells up-regulated *grp78* mRNA levels by 6–7-fold when treated with 0.75 µM TN (Fig. 5). Thus, although ER Ca^{2+} pool depletion failed to induce an up-regulation of *grp78* mRNA, accumulation of unglycosylated proteins in the ER induced a strong up-regulation of *grp78* mRNA levels. These findings suggest that there is more than one signal transduction pathway for *grp78* induction (see "Discussion").

To assess if *grp94* is regulated in the same manner as *grp78* in WEHI7.2 and W.Hb12 cells, we examined the steady-state level of *grp94* mRNA after treatment with 100 nM TG (Fig. 6). A modest elevation of *grp94* mRNA levels appeared to occur at 5 h after TG addition in both WEHI7.2 and W.Hb12 cells. In multiple experiments, however, the maximum ratio of post-treatment to pretreatment *grp94* mRNA levels in WEHI7.2 cells was only 2.0 ± 0.5, which did not represent a reproducible elevation above base-line levels ($p \geq 0.05$). In W.Hb12 cells, the maximum ratio was only 1.5 ± 0.2, which also did not represent a significant elevation above base-line levels ($p \geq 0.05$).

The preceding findings suggest that TG treatment does not signal an increase in *grp78/grp94* transcription in the WEHI7.2
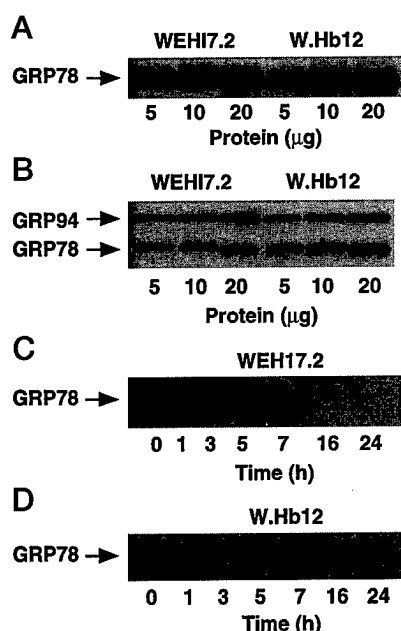
Deficient grp78/grp94 Stress Response

A

GRP78 →

WEHI7.2   W.Hb12

5 10 20 5 10 20
Protein (µg)

B

GRP94 →
GRP78 →

WEHI7.2   W.Hb12

5 10 20 5 10 20
Protein (µg)

C

GRP78 →

WEH17.2

0 1 3 5 7 16 24
Time (h)

D

GRP78 →

W.Hb12

0 1 3 5 7 16 24
Time (h)

FIG. 4. **GRP78 and GRP94 protein levels in WEHI7.2 and W.Hb12 cells.** *A* and *B*, protein was isolated from exponentially growing cells and separated by SDS-polyacrylamide gel electrophoresis in the amounts shown. Western blots were probed with a monoclonal antibody to GRP78 (*A*) or with a polyclonal antibody that recognizes both GRP94 and GRP78 (*B*). *C* and *D*, protein, isolated from WEHI7.2 and W.Hb12 cells, respectively, at various times after adding 100 nM TG, was separated by SDS-polyacrylamide gel electrophoresis and analyzed by Western blotting using a monoclonal antibody to GRP78.
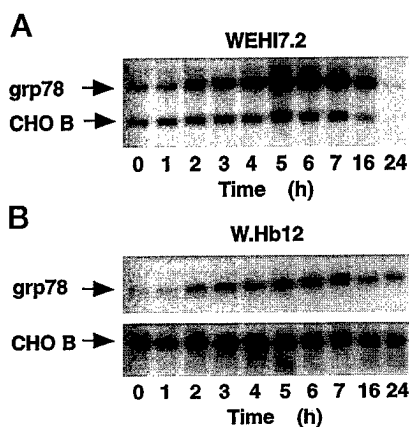

A

grp78 →
CHO B →

WEHI7.2

0 1 2 3 4 5 6 7 16 24
Time (h)

B

grp78 →
CHO B →

W.Hb12

0 1 2 3 4 5 6 7 16 24
Time (h)

FIG. 5. **Effect of TN treatment on** *grp78* **mRNA levels in WEHI7.2 and W.Hb12 cells.** Exponentially growing cells were diluted to a concentration of 1 × 10⁶/ml with fresh culture medium before adding 0.75 µM TN. RNA was isolated at the indicated times following TN addition and analyzed by Northern hybridization using radiolabeled *grp78* and CHO-B cDNA probes. Representative blots for WEHI7.2 cells (*A*) and W.Hb12 cells (*B*) are shown.

A

grp94 →
CHO B →

WEHI7.2

0 1 3 5 7 16 24
Time (h)

B

grp94 →
CHO B →

W.Hb12

0 1 3 5 7 16 24
Time (h)

FIG. 6. **Effect of TG treatment on** *grp94* **mRNA levels in WEHI7.2 and W.Hb12 cells.** Exponentially growing cells were diluted to a concentration of 1 × 10⁶/ml with fresh culture medium before adding 100 nM TG. RNA was isolated at the indicated times following TG addition and analyzed by Northern hybridization using radiolabeled *grp94* and CHO-B cDNA probes. Representative blots for WEHI7.2 cells (*A*) and W.Hb12 cells (*B*) are shown.

A

WEHI7.2 TG   WEHI7.2 TN

grp78 →
grp94 →
CHO B →
pBR322 →

0   5   7   0   5   7
Time (h)

B

W.Hb12 TG   W.Hb12 TN

grp78 →
grp94 →
CHO B →
pBR322 →

0   5   7   0   5   7
Time (h)

FIG. 7. **Effect of TG and TN treatment on** *grp78* **and** *grp94* **transcription.** Nuclei were isolated from WEHI7.2 cells (*A*) and W.Hb12 cells (*B*) after treatment with 100 nM TG or 0.75 µM TN for the indicated times. Equal amounts (cpm) of ³²P-labeled nuclear run-off RNA were hybridized to slot blots containing 5 µg of immobilized *grp78* or *grp94* plasmids. Hybridization of run-off RNA to slot blots containing the CHO-B plasmid and the empty plasmid vector pBR322 was used as a control. The time samples taken following TG or TN addition are indicated. Results are representative of three experiments.

lymphoma cell line or its derivatives that express Bcl-2. To confirm that this is the case, we measured the effect of TG treatment on the transcription rate of *grp78* and *grp94* genes by nuclear run-off assays using isolated nuclei from WEHI7.2 and W.Hb12 cells. An increase in newly expressed *grp78/grp94* message after TG treatment was not detected in WEHI7.2 cells (Fig. 7*A*) or W.Hb12 cells (Fig. 7*B*). TN treatment, however, did induce a significant increase in *grp78* and *grp94* transcription, which was detected by 5 and 7 h, respectively. This indicates that *grp78/grp94* transcription is not induced by TG in WEHI7.2 cells or derivatives that express Bcl-2, but is induced by TN.

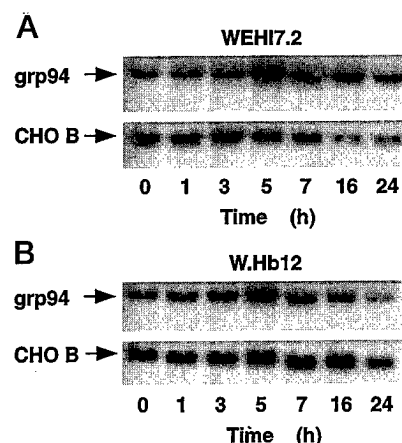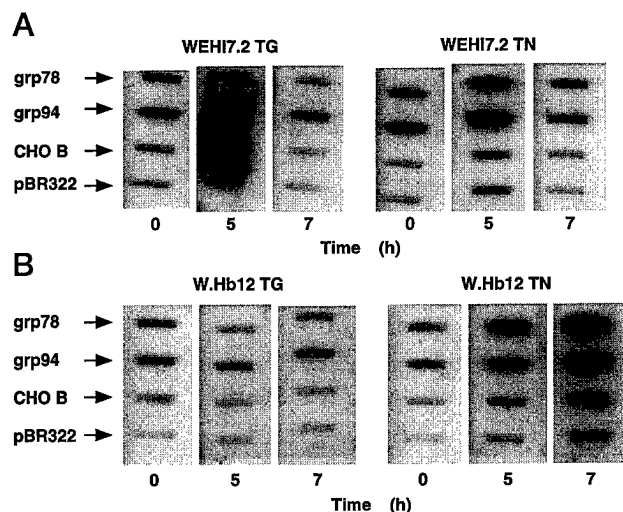Because earlier studies of *grp78* regulation have emphasized

epithelial cells and fibroblasts (see the Introduction), as a positive control, we examined the effect of TG treatment on *grp78* mRNA levels in three epithelial breast cancer lines, Mm5MT, MDA-MB-468, and MCF-7. Treatment of Mm5MT cells with 100 nM TG did not induce cell death (Fig. 8*D*), but did induce a 5-fold elevation of *grp78* mRNA levels detectable within 7 h of adding TG (Fig. 8*B*). MDA-MB-468 and MCF-7 cells were also much less sensitive than WEHI7.2 cells to TG-induced cell death (Fig. 8*D*) and displayed marked induction of *grp78* mRNA levels in response to TG treatment (Fig. 8, *B* and *C*).

To determine if the defect in TG-mediated *grp78* signaling is observed in other lymphoid cells, we measured the effect of TG treatment on *grp78* mRNA levels in two additional Bcl-2-negative mouse lymphoma lines, W7.MG1 and S49.1. *grp78* transcription is induced by TN treatment in both of these lines (31). The level of *grp78* mRNA failed to increase following TG treatment in W7.MG1 cells, which rapidly lost viability following TG
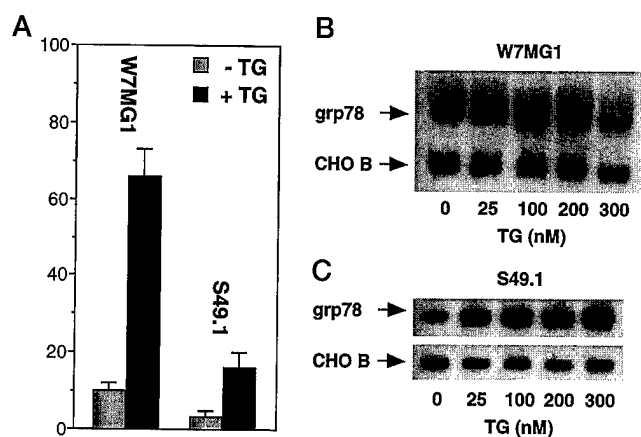
A

B

C

D
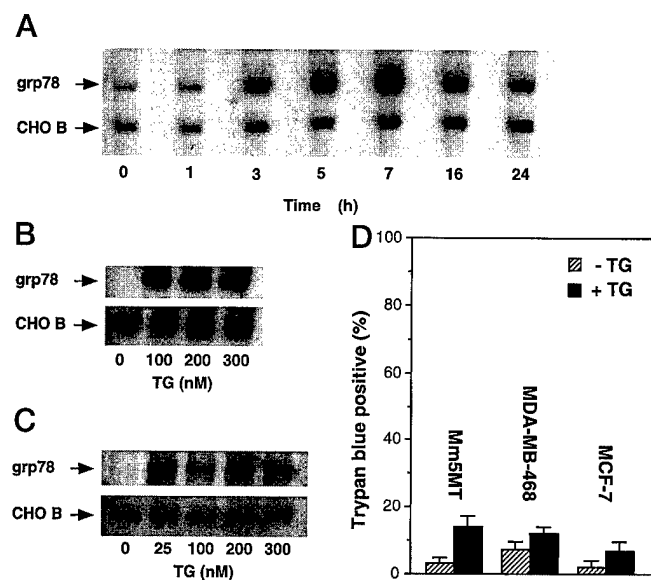
FIG. 8. **Effect of TG on** *grp78* **mRNA levels and viability in breast cancer cells.** *A*, exponentially growing Mm5MT cells were treated with 100 nM TG. RNA was isolated at the indicated times following TG addition and analyzed by Northern hybridization using radiolabeled *grp78* and CHO-B cDNA probes. *B*, exponentially growing MDA-MB-468 cells were treated with multiple concentrations of TG. RNA was isolated 7 h after TG addition and analyzed by Northern hybridization using radiolabeled *grp78* and CHO-B cDNA probes. *C*, exponentially growing MCF-7 cells were treated with multiple concentrations of TG. RNA was isolated 7 h after TG addition and analyzed by Northern hybridization using radiolabeled *grp78* and CHO-B cDNA probes. *D*, exponentially growing cells were incubated for 24 h in the presence or absence of 100 nM TG. The percentage of trypan blue-positive cells was measured 24 h after TG addition. *Error bars* represent the mean of duplicate determinations in multiple experiments.

treatment, whereas the level of *grp78* mRNA did increase 3–4-fold following TG treatment in S49.1 cells, which were relatively resistant to TG-induced cell death (Fig. 9). These data are consistent with the concept that a deficiency of *grp78* induction increases susceptibility to TG-induced cell death.

DISCUSSION

We have discovered that the transcription of *grp78* and *grp94* is not significantly increased in WEHI7.2 cells in response to treatment with the ER Ca^{2+}-ATPase inhibitor TG, even when apoptosis is inhibited by overexpressing grp78. Examination of two additional lymphoma lines revealed an absence of *grp78* induction in W7.MG1 cells and 3–4-fold induction of *grp78* in S49.1 cells following TG treatment. By comparison, TG treatment induced a marked elevation of *grp78* mRNA levels in all three nonlymphoid lines tested (Mm5MT, MDA-MB-468, and MCF-7), consistent with studies indicating that TG treatment substantially induces *grp78/grp94* transcription in epithelial cells and fibroblasts (13).

We have previously shown, in WEHI7.2 cells and derivatives expressing Bcl-2, that TG treatment inhibits the ER Ca^{2+}-ATPase, producing cytosolic Ca^{2+} elevation and ER Ca^{2+} pool depletion (30, 36). Hence, the failure to significantly elevate *grp78/grp94* transcription following TG treatment is not due to a failure of TG to disrupt Ca^{2+} homeostasis. Moreover, in the present study, we show that TN treatment induces a substantial *grp78/grp94* transcriptional response. This observation is important for two reasons. First, it provides evidence that the *grp78/grp94* stress response is not already maximally induced in WEHI7.2 cells. Second, it suggests that the *grp78/grp94* stress response induced by Ca^{2+} mobilization may be regulated differently than that induced by TN. Ca^{2+} mobilization and inhibition of glycosylation have been shown to induce *grp78/*

A

B

C

FIG. 9. **Effect of TG on** *grp78* **mRNA levels and viability in lymphoma cells.** *A*, exponentially growing cells were incubated for 24 h in the presence or absence of 100 nM TG. The percentage of trypan blue-positive cells was measured 24 h after TG addition. *Error bars* represent the mean of duplicate determinations in multiple experiments. *B*, exponentially growing W7.MG1 cells were diluted to a concentration of 0.5 × 10^6/ml in fresh culture medium 7 h before adding 100 nM TG. RNA was isolated 7 h after TG addition and analyzed by Northern hybridization using radiolabeled *grp78* and CHO-B cDNA probes. *C*, exponentially growing S49.1 cells were diluted to a concentration of 0.5 × 10^6/ml in fresh culture medium 7 h before adding 100 nM TG. RNA was isolated 7 h after TG addition and analyzed by Northern hybridization using radiolabeled *grp78* and CHO-B cDNA probes.

grp94 transcription through common promoter elements (12). Therefore, the deficiency in the TG-induced *grp78/grp94* transcriptional response observed in WEHI7.2 cells is unlikely to reside at the promoter level. One possible explanation for our findings is that two independent ER-to-nucleus *grp78/grp94* signaling pathways may exist: one Ca^{2+}-mediated and the other mediated by glycosylation inhibition. Both pathways are operative in fibroblasts and epithelial cells, which induce *grp78/grp94* in response to both TG and TN, but only the glycosylation inhibition signaling pathway appears to be operative in WEHI7.2 cells.

Little is known about the ER-to-nucleus signaling pathway that activates *grp78/grp94* transcription. ER-to-nucleus signaling may be Ca^{2+}/calmodulin-regulated (37) or may be mediated through tyrosine kinases and/or serine/threonine kinases (38, 39). Recently, it has been shown that IRE1p (Ern1), a yeast transmembrane serine/threonine kinase required for the induction of *KAR2*, the yeast homologue of *grp78*, may play a role in the ER-to-nucleus signaling pathway mediating *KAR2/grp78* up-regulation in response to malfolded proteins (40, 41). Overexpression of IRE1p in fibroblasts produced a modest increase in the ability of transfectants to up-regulate *grp78* in response to TG treatment (39). The WEHI7.2 cell line described in this report may be a useful model for the delineation of ER-to-nucleus signaling pathways. For example, it will be interesting to determine whether or not expression of IRE1p/Ern1 restores Ca^{2+}-mediated *grp78/grp94* transcriptional induction in these cells, thus further elucidating the role of IRE1p/Ern1 proteins in the pathway of *grp78/grp94* induction.

Understanding ER-to-nucleus signaling pathways should provide insight into mechanisms that regulate apoptosis induction during ER Ca^{2+} pool depletion. Indeed, our findings suggest that cells deficient in *grp78* stress response signaling are more susceptible to TG-induced apoptosis than cells that mount a *grp78* stress response. These findings are consistent with those of earlier work by Lee and co-workers (26–28) in fibroblasts and epithelial cells, indicating that up-regulation of *grp78* and coordinately regulated *grp94*, in response to ER Ca^{2+} pool depletion, prevents cell death. Hence, when the

grp78/grp94 response was inhibited, fibroblasts died in response to treatment with agents that mobilize Ca^{2+} from the ER, including TG and the Ca^{2+} ionophore A23187. Using a *grp78* antisense plasmid, they demonstrated that the inability to up-regulate *grp78* resulted in increased cell death following A23187 treatment (26). Similarly, when *grp78* induction was inhibited by amplification of the *grp78* core promoter region, an increased sensitivity to A23187 was observed (27). Furthermore, when induction of *grp78/grp94* was inhibited by ribozyme cleavage of newly transcribed *grp94* mRNA, increased sensitivity to A23187 and TG was observed (28). Interestingly, abrogation of the *grp78/grp94* stress response did not enhance the cytotoxicity of TN, suggesting that the increase in *grp78/grp94* transcription provides specific protection against ER Ca^{2+} pool depletion (28). In agreement with their findings, we have found that WEHI7.2 and W.Hb12 cells were killed by TN (data not shown), even though TN increased *grp78/grp94* transcription.

Understanding the role of *grp78/grp94* in regulating cell death may have important implications for cancer therapy. In this regard, there is evidence that prior induction of *grp78* can make cells less susceptible to death following treatment with photodynamic therapy (42), the superoxide-generating anticancer agent doxorubicin (43), and the topoisomerase inhibitor etoposide (44).

In summary, the findings reported here have three important implications. First, the *grp78/grp94* stress response may be differentially regulated among different types of cells, with a much greater response observed in nonlymphoid cells than in lymphoid cells. Second, there may be at least two signal transduction pathways that mediate the *grp78/grp94* stress response, one in response to ER Ca^{2+} mobilization and the other in response to protein glycosylation inhibition. Third, regulation of the *grp78/grp94* stress response may be a major factor in deciding whether a cell lives or dies in response to disruption of intracellular Ca^{2+} homeostasis. Indeed, the absence of a Ca^{2+}-mediated *grp78/grp94* stress response may be the basis for the marked susceptibility of WEHI7.2 cells to TG-induced apoptosis.

REFERENCES

1. Sambrook, J. F. (1990) *Cell* **61**, 197–199
2. Lodish, H. F., Kong, N., and Wikstrom, L. (1992) *J. Biol. Chem.* **267**, 12753–12760
3. Gething, M.-J., and Sambrook, J. (1992) *Nature* **355**, 33–45
4. Brostrom, C. O., and Brostrom, M. A. (1990) *Annu. Rev. Physiol.* **52**, 577–590
5. Koch, G., Smith, M., Macer, D., Webster, P., and Mortara, R. (1986) *J. Cell Sci.* **86**, 217–232
6. Booth, C., and Kock, G. L. E. (1989) *Cell* **59**, 729–737
7. Short, A. D., Bian, J., Ghosh, T. K., Waldron, R. T., and Rybak, S. L. (1993) *Proc. Natl. Acad. Sci. U. S. A.* **90**, 4986–4990
8. Thastrup, O., Cullen, P. J., Drobak, B. K., Hanley, M. R., and Dawson, A. P. (1990) *Proc. Natl. Acad. Sci. U. S. A.* **87**, 2466–2470
9. Lytton, J., Westlin, M., and Hanley, M. R. (1991) *J. Biol. Chem.* **266**, 17067–17071
10. Lee, A. S. (1987) *Trends Biol. Sci.* **12**, 20–23
11. Mazzarella, R. A., and Green, M. (1987) *J. Biol. Chem.* **262**, 8875–8883
12. Wooden, S. K., Li-Jing, L., Navarro, D., Qadri, I., Pereira, L., and Lee, A. S. (1991) *Mol. Cell. Biol.* **11**, 5612–5622
13. Little, E., Ramakrishnan, M., Roy, B., Gazit, G., and Lee, A. S. (1994) *Crit. Rev. Eukaryotic Gene Expression* **4**, 1–18
14. Kim, Y. K., Kim, K. S., and Lee, A. S. (1987) *J. Cell. Physiol.* **133**, 533–559
15. Bole, D. G., Hendershot, L. M., and Kearney, J. F. (1986) *J. Cell Biol.* **102**, 1558–1566
16. Hunt, C., and Morimoto, R. I. (1985) *Proc. Natl. Acad. Sci. U. S. A.* **82**, 6455–6459
17. Sanders, S. L., Whitfield, K. M., Vogel, J. P., Rose, M. D., and Schekman, R. W. (1992) *Cell* **69**, 353–365
18. Dorner, A. J., Krane, M. G., and Kaufman, R. J. (1988) *Mol. Cell. Biol.* **8**, 4063–4070
19. Dorner, A. J., Wasley, L. C., and Kaufman, R. J. (1992) *EMBO J.* **11**, 1563–1571
20. Machamer, C. E., Doms, R. W., Bole, D. G., Helenius, A., and Rose, J. K. (1990) *J. Biol. Chem.* **265**, 6879–6883
21. Hendershot, L. M., Ting, J., and Lee, A. S. (1988) *Mol. Cell. Biol.* **8**, 4250–4256
22. Melnick, J., Dul, L., and Argon, Y. (1994) *Nature* **370**, 373–375
23. Li, Z., and Srivastava, P. K. (1993) *EMBO J.* **12**, 3143–3151
24. Kozutsumi, Y., Segal, M., Normington, K., Gething, M.-J., and Sambrook, J. (1988) *Nature* **332**, 462–464
25. Li, W. W., Alexandre, S., Cao, X., and Lee, A. S. (1993) *J. Biol. Chem.* **268**, 12003–12009
26. Li, L., Li, X., Ferrario, A., Rucker, N., Liu, E. S., Wong, S., Gomer, C. J., and Lee, A. S. (1992) *J. Cell. Physiol.* **153**, 575–582
27. Li, X., and Lee, A. S. (1991) *Mol. Cell. Biol.* **11**, 3446–3453
28. Little, E., and Lee, A. S. (1995) *J. Biol. Chem.* **270**, 9526–9534
29. Brostrom, M. A., Cade, C., Prostko, C. R., Gmitter-Yellen, D., and Brostrom, C. O. (1990) *J. Biol. Chem.* **265**, 20539–20546
30. Lam, M., Dubyak, G., Chen, L., Nunez, G., Miesfeld, R. L., and Distelhorst, C. W. (1994) *Proc. Natl. Acad. Sci. U. S. A.* **91**, 6569–6573
31. Ulatowski, L. M., Lam, M., Vanderburg, G., Stallcup, M. R., and Distelhorst, C. W. (1993) *J. Biol. Chem.* **268**, 7482–7488
32. Lenny, N., and Green, M. (1991) *J. Biol. Chem.* **266**, 20532–20537
33. Greenberg, M. E., and Bender, T. P. (1994) *Current Protocols in Molecular Biology* (Ausubel, F. M., Brent, R., Kingston, R. E., Moore, D. D., Seidman, J. G., Smith, J. A., and Struhl, K., eds) pp. 4.10.1–4.10.11, Greene Publishing Associates/Wiley-Interscience, New York
34. Lofquist, A. K., Mondal, K., Morris, J. S., and Haskill, J. S. (1995) *Mol. Cell. Biol.* **15**, 1737–1746
35. Fei, H., and Drake, T. A. (1993) *BioTechniques* **15**, 838
36. Distelhorst, C. W., and McCormick, T. S. (1996) *Cell Calcium* **19**, 473–483
37. Resendez, E., Ting, J., Kim, K. S., Wooden, S. K., and Lee, A. S. (1986) *J. Cell Biol.* **103**, 2145–2152
38. Price, B. D., and Calderwood, S. K. (1992) *Cancer Res.* **52**, 3814–3817
39. Cao, X., Zhou, Y., and Lee, A. S. (1995) *J. Biol. Chem.* **270**, 494–502
40. Mori, K., Ma, W., Gething, M.-J., and Sambrook, J. (1993) *Cell* **74**, 743–756
41. Cox, J. S., Shamu, C. E., and Walter, P. (1993) *Cell* **73**, 1197–1206
42. Gomer, C. J., Ferrario, A., Rucker, N., Wong, S., and Lee, A. S. (1991) *Cancer Res.* **51**, 6574–6579
43. Shen, J., Hughes, C., Chao, C., Cai, J., Bartels, C., Gessner, T., and Subjeck, J. (1987) *Proc. Natl. Acad. Sci. U. S. A.* **84**, 3278–3282
44. Hughes, C. S., Shen, J. W., and Subjeck, J. R. (1989) *Cancer Res.* **49**, 4452–4454

Baculovirus p35 and Z-VAD-fmk inhibit thapsigargin-induced apoptosis of breast cancer cells

Xiao-Mei Qi, Huiling He, Hongying Zhong and Clark W Distelhorst

Department of Medicine, Case Western Reserve University/Ireland Cancer Center, Cleveland, Ohio 44106, USA

Programmed cell death, or apoptosis, is inhibited by the antiapoptotic oncogene, Bcl-2, and is mediated by a cascade of aspartate-specific cysteine proteases, or caspases, related to interleukin 1-β converting enzyme. Depending on cell type, apoptosis can be induced by treatment with thapsigargin (TG); a selective inhibitor of the endoplasmic reticulum-associated calcium-ATPase. The role of caspases in mediating TG-induced apoptosis was investigated in the Bcl-2-negative human breast cancer cell line, MDA-MB-468. Apoptosis developed in MDA-MB-468 cells over a period of 24–72 h following treatment with 100 nM TG, and was prevented by Bcl-2 overexpression. TG-induced apoptosis was associated with activation of caspase-3 and was inhibited by stable expression of the baculovirus p35 protein, an inhibitor of caspase activity. Also, TG-induced apoptosis was inhibited by treating cells with Z-VAD-fmk, a cell-permeable fluoromethylketone inhibitor of caspases. These findings indicate that TG-induced apoptosis of MDA-MB-468 breast cancer cells is subject to inhibition by Bcl-2 and is mediated by caspase activity. This model system should be useful for further investigation directed toward understanding the role of calcium in signaling apoptosis, and its relationship to Bcl-2 and the caspase proteolytic cascade.

Keywords: thapsigargin; apoptosis; Bcl-1; ICE-like protease

Introduction

Programmed cell death (PCD), or apoptosis, is important for proper development and homeostasis of tissues; thus, insight into PCD mechanisms will contribute to improved understanding and treatment of diseases in which the normal balance between cell proliferation and cell death is disrupted (Thompson, 1995). For example, the PCD process mediates both the physiologic involution of normal breast epithelium following lactation and the regression of breast cancer following hormonal manipulation or chemotherapy administration (McCloskey *et al.*, 1996).

Studies in the primitive nematode, *C. elegans*, have contributed considerably to our understanding of fundamental PCD mechanisms by proving that apoptosis involves a systematic, stepwise process of cellular destruction regulated by genes encoding either death inhibitors or effectors (Steller, 1995). For example, the *C. elegans* gene ced-9 encodes an inhibitor of cell death, whereas the ced-3 and ced-4 genes encode death effectors. Mammalian cells express genes homologous to ced-9 and ced-3, indicating that the apoptotic pathway is highly conserved. The mammalian homolog of ced-9 is bcl-2, a potent inhibitor of apoptosis that prevents PCD triggered by diverse death signals (Cory, 1995). The mammalian homolog of ced-3 is the cysteine protease, interleukin 1-β converting enzyme (ICE) (Yuan *et al.*, 1993). ICE, along with a number of ICE-like proteases, or caspases, compose a family of cysteine proteases that cleave proteins at aspartic acid residues (Henkart, 1996). Recent findings suggest that a caspase proteolytic cascade mediates cell death by cleaving selected target proteins (Martin and Green, 1995; Fraser and Evan, 1996). Bcl-2 appears to inhibit apoptosis by preventing caspase activation Chinnaiyan *et al.*, 1996; Jacobson *et al.*, 1996; Shimizu *et al.*, 1996). ICE-like proteases have been implicated as mediators of apoptosis in response to a variety of death signals, including trophic factor deprivation, protein kinase inhibition by staurosporine, and cytotoxic lymphocyte killing (Milligan *et al.*, 1995; Jacobson *et al.*, 1996; Martin *et al.*, 1996). Thus, activation of a caspase cascade may be a final common pathway where diverse cell death signals converge.
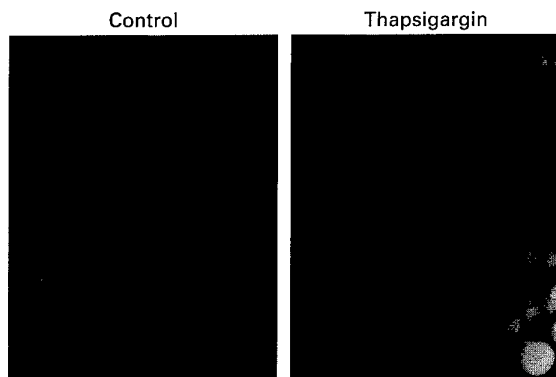
We have been investigating the mechanism of cell death signaling following inhibition of calcium ion uptake into the endoplasmic reticulum (ER) by the sesqueterpene lactone tumor promoter thapsigargin (TG). In lymphoma cells, TG treatment induces apoptotic cell death, which can be prevented by Bcl-2 overexpression (Lam *et al.*, 1993, 1994). In the present report, we show that TG also induces apoptosis in the human breast cancer cell line, MDA-MB-468, and that TG-induced apoptosis involves caspase-3 activation and is prevented by expressing the baculovirus antiapoptotic protein p35, an inhibitor of caspases (Bump *et al.*, 1995). Also, we show that TG-induced apoptosis can be inhibited by treating cells with a cell-permeable, irreversible, tripeptide inhibitor of caspases, Z-Val-Ala-Asp-fluoromethylketone (Z-VAD-fmk) (Jacobson *et al.*, 1996). These findings indicate that TG-induced apoptosis is mediated through a highly conserved PCD process regulated by Bcl-2 and mediated by caspases.

Results

When treated with 100 nM TG, MDA-MB-468 cells underwent apoptotic cell death. The distinction between viable cells and apoptotic cells was based on nuclear chromatin pattern, assessed by fluorescence microscopy of cells stained with acridine orange (Figure 1). The nuclear chromatin of viable cells was

dispersed, whereas that of apoptotic cells was condensed into densely fluorescent apoptotic bodies. To test the effect of Bcl-2 on TG-induced apoptosis, MDA-MB-468 cells were stably transfected with pSFFV-neo-Bcl-2 or pSFFV-neo, producing 468-Bcl-2 and 468-neo cells, respectively. Bcl-2 was present at very low levels in 468-neo cells, but was readily detected by Western blotting in 468-Bcl-2 cells (Figure 2a). Following exposure to 100 nM TG, 468-neo cells underwent apoptosis, which evolved over a period of 24–72 h (Figure 2b). Thus, the kinetics of apoptosis induction were much slower than reported previously in lymphoma cells, where a peak in the percentage of apoptotic cells was detected within 12 h of adding 100 nM TG (McCormick et al., 1997). TG-induced apoptosis was markedly repressed in 468-Bcl-2 cells, representative of multiple Bcl-2-expressing clones, indicating that TG-induced apoptosis is mediated through a Bcl-2-regulated pathway (Figure 2b).
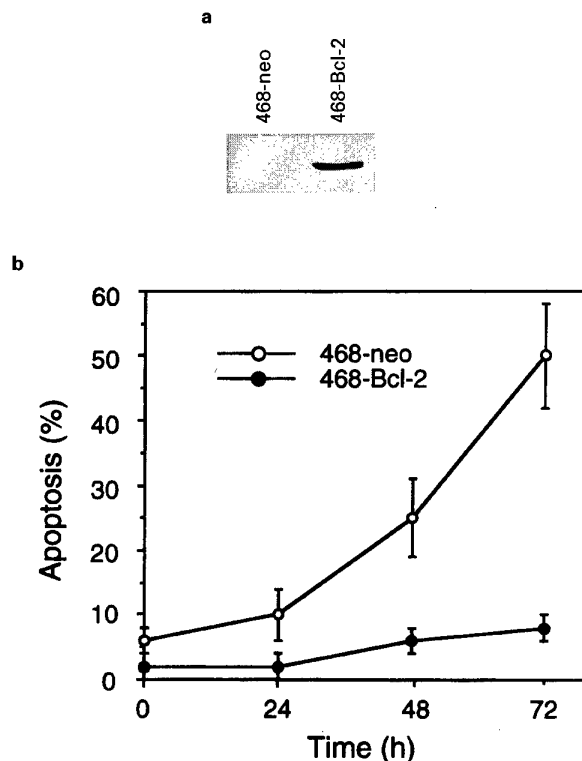
To determine if TG-induced apoptosis is associated with caspase activation, the level of pro-caspase-3 (CPP32, Yama, or apopain) was assessed in MDA-MB-468 cells by Western blotting using a monoclonal antibody to human pro-caspase-3. During activation, pro-caspase-3 undergoes cleavage to two subunits that form the active heterotetramer (Henkart, 1996). The level of pro-caspase-3 declined within 48 h of TG addition, indicating conversion of pro-caspase-3 to an active form (Figure 3). Two methods were employed to determine whether or not ICE-like protease activation is a necessary step in TG-induced apoptosis. In the first, MDA-MB-468 cells were stably transfected with the pSFFV-neo expression vector into which the cDNA encoding p35, a baculovirus inhibitor of ICE-like proteases, had been cloned. Cells stably transfected with this vector are referred to as 468-p35 cells, while cells stably transfected with empty vector alone are referred to as 468-neo cells. p35 mRNA was detected by Northern hybridization in two 468-p35 subclones (1 and 4), but not in 468-neo cells (Figure 4). On light microscopy, healthy 468-neo cells have a somewhat elongated appearance and are adherent to plastic tissue

culture wells, whereas apoptotic cells have a small rounded appearance and are non-adherent (Figure 5). Following treatment of 468-neo cells with TG, there was a marked increase in the proportion of apoptotic cells. Untreated 468-p35 cells have an appearance similar to that of 468-neo cells, except that fewer spontaneously apoptotic cells were observed in culture. In addition, fewer apoptotic cells were detected in cultures of 468-p35 cells following TG treatment compared to TG-treated cultures of 468-neo cells. To corroborate these findings, the percentage of apoptotic cells following TG treatment was quantitated by fluorescence microscopy (Figure 6a). The data confirm the inhibition of TG-induced apoptosis by p35.

In a second approach, cells were treated with TG in the presence or absence of the peptide fluoromethylk-etone inhibitor Z-VAD-fmk. The tripeptide sequence in Z-VAD-fmk corresponds to the P_1 to P_3 residues of the pro-IL-1β cleavage site (Tyr^{4}ValAlaAsp^{1}Gly), where ICE cleaves between the Asp and Gly residue (Yuan et al., 1993). Deletion of the Tyr residue broadens the inhibitory spectrum to include not only ICE, but other proteases closely related to ICE. An effective treatment regimen was empirically derived in which cells were treated with 200 μM doses of Z-VAD-fmk added 1 h prior to TG, and every 12 h thereafter over a period of 48 h. Z-VAD-fmk had a marked inhibitory effect on

a

468-neo   468-Bcl-2

b

Figure 1 TG induces apoptosis of MDA-MB-468 cells. Cells in exponential phase of cell growth were treated with 100 nM TG dissolved in DMSO. A replicate cell culture, treated with an equivalent amount of DMSO, served as a control. Nuclear morphology of cells stained with ethidium bromide and acridine orange was visualized by fluorescence microscopy 48 h after adding TG or DMSO. Small dense fluorescent bodies seen in TG-treated cells represent nuclear chromatin condensation characteristic of apoptosis

Figure 2 Inhibition of TG-induced apoptosis by Bcl-2. (a) Protein was isolated from MDA-MB-468 cells that had been stably transfected with pSFFV-neo (468-neo) or pSFFV-neo-Bcl-2 (468-Bcl-2). Protein (50 μg) was resolved by SDS–PAGE and analysed by Western blotting using a Bcl-2 monoclonal primary antibody. (b) The percentage of 468-neo and 468-Bcl-2 cells with an apoptotic nuclear morphology at various times after adding 100 nM TG was measured by fluorescence microscopy as described in Figure 1. Symbols represent the mean±s.e. of four experiments

Control   Thapsigargin

a

b
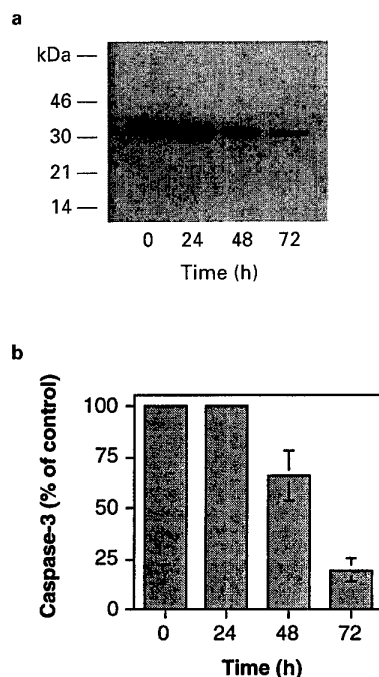
Figure 3 Caspase-3 activation by TG. (a) Protein was isolated from MDA-MB-468 cells at time intervals following addition of 100 nM TG and subjected to Western blotting to detect the level of caspase-3 (CPP32/Yama/Apopain). (b) The level of caspase-3 on Western blots was measured by densitometry. Symbols represent the mean±s.e. of three experiments
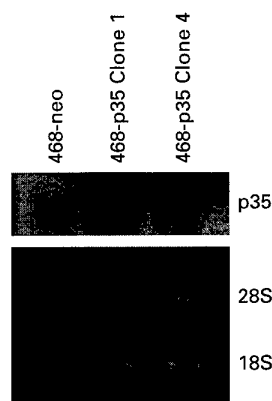

Figure 4 Northern blot analysis of p35 mRNA in MDA-MB-468 cells. RNA was isolated from MDA-MB-468 cells that had been transfected with pSFFV-neo (468-neo) and pSFFV-neo-p35 (468-p35, clones 1 and 4), and analysed by Northern hybridization using a cDNA probe for p35 (top panel). The bottom panel shows ethidium bromide-stained 28S and 18S rRNA from each sample, indicating equivalent RNA loading

TG-induced apoptosis (Figure 6b), whereas Z-FA-fmk, a cathepsin inhibitor, actually induced cell death (data not shown).

Discussion

In experiments reported here, we found that TG treatment induces apoptosis of MDA-MB-468 cells, an estrogen receptor negative human breast cancer cell line that has been employed by others to investigate
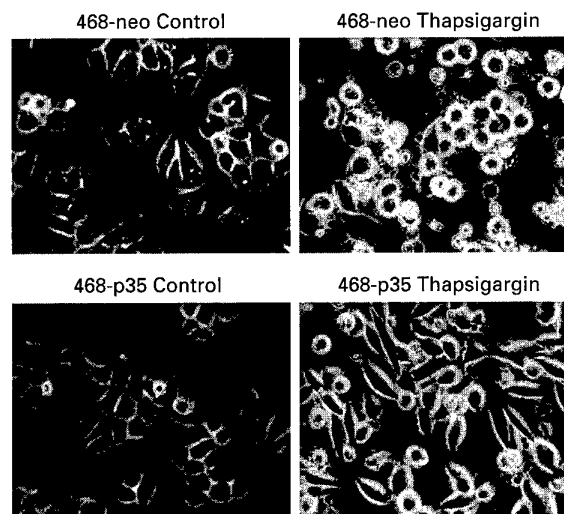
Figure 5 Effect of baculovirus p35 on TG-induced cell death. MDA-MB-468 transfectants, 468-neo and 468-p35 (clone 1), were treated with either 100 nM TG dissolved in DMSO or an equivalent volume of DMSO (control). Shown are photographs of the cells 48 h after treatment was initiated

PCD in breast cancer (Armstrong et al., 1992, 1994). Our findings add to the number of recognized cell types in which TG treatment induces apoptosis, including normal thymocytes (Jiang et al., 1994), lymphoma cells (Lam et al., 1993, 1994) and prostate carcinoma cells (Furuya et al., 1994). However, not all cell types readily undergo apoptosis following TG treatment. For example, smooth muscle cells, fibroblasts and epithelial cells have been reported to undergo growth arrest, without loss of viability, following TG treatment (Ghosh et al., 1989; Li et al., 1993). In the case of smooth muscle cells, survival in the presence of TG is mediated through induction of TG-insensitive calcium pumps that restore calcium homeostasis within the ER lumen (Waldron et al., 1995); whereas in the case of fibroblasts and epithelial cells, maintenance of cell viability following TG treatment is dependent upon the induction of the grp78 and grp94 genes encoding the resident ER calcium-binding proteins, GRP78 and GRP94 respectively (Li et al., 1993). Moreover, the rate of cell death induction following TG treatment also varies among different types of cells. For example, in lymphoma cells, TG treatment induces rapid onset of apoptosis within less than 12 h; whereas, as shown in the present study, induction of apoptosis in breast cancer cells evolves more slowly following TG treatment. In part, the kinetics of cell death induction in TG-treated cells may depend upon the magnitude of grp78/grp94 induction, a concept based on the observation that grp78/grp94 induction is detected in TG-treated breast cancer cells, but not in TG-treated lymphoma cells (McCormick et al., 1997).

The mechanism of apoptosis induction by TG is not fully understood, but appears to be directly related to inhibition of ER calcium-ATPase activity, which produces sustained elevation of cytosolic calcium and sustained depletion of the ER calcium pool (Thastrup et al., 1990). Apoptosis induction may be signaled in response to cytosolic calcium elevation, consistent with evidence that factors interfering with cytosolic calcium elevation inhibit TG-induced apoptosis (Jiang et al.,

A

B
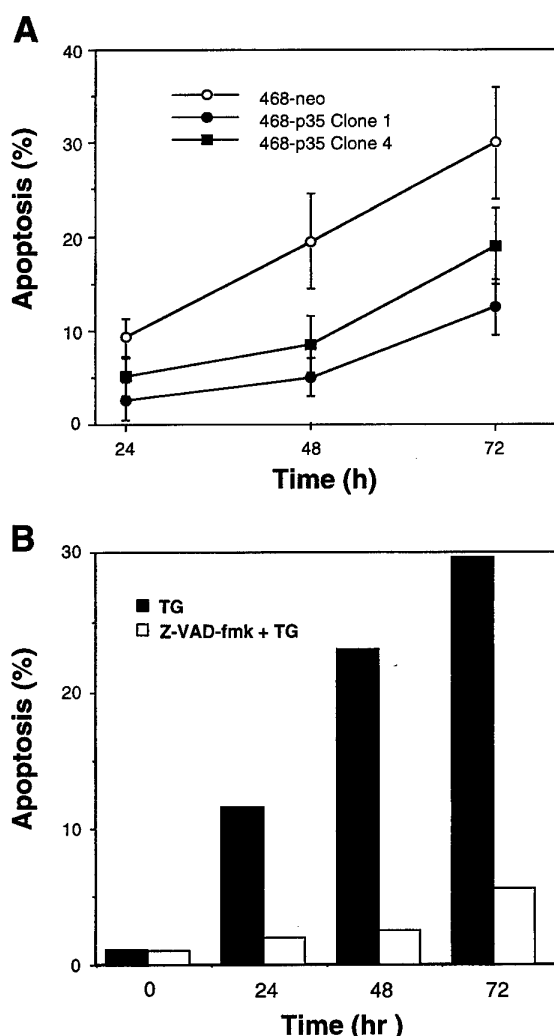
Figure 6 Effect of baculovirus p35 and Z-VAD-fmk on TG-induced apoptosis. (a) MDA-MB-468 transfectants, 468-neo and 468-p35 (clones 1 and 4), were treated with 100 nM TG. The percentage of cells with an apoptotic nuclear morphology was determined by fluorescence microscopy at the indicated times after adding TG. Symbols represent the mean±s.e. of multiple cell counts in two separate experiments. (b) MDA-MB-468 cells were treated with 100 nM TG in the presence or absence of Z-VAD-fmk. TG (100 nM) was added to cells at time 0. Z-VAD-fmk (200 μM) was added to one set of cells 1 h before adding TG and at 12, 24, and 36 h thereafter. The percentage of cells with an apoptotic nuclear morphology was determined by fluorescence microscopy at the indicated time points after adding TG. Symbols represent the mean of multiple determinations in a single experiment that was repeated once with the same result

branes (Lam et al., 1994), a concept that is intriguing in view of recent evidence that Bcl-XL, a Bcl-2 homolog, has a structure consistent with that of an ion channel (Muchmore et al., 1996).

The present report extends our understanding of TG-induced apoptosis by providing evidence of involvement of ICE-like proteases. One type of evidence is the inhibition of TG-induced apoptosis by baculovirus p35, an inhibitor of a number of ICE-family proteases (Bump et al., 1995). Expression of p35 has been used by others to document the involvement of ICE-like proteases in mediating PCD in insect cells (Cartier et al., 1994), C. elegans (Sugimoto et al., 1994), Drosophila (Hay et al., 1994), and mammalian cells (Rabizadeh et al., 1993; Beidler et al., 1995). Therefore, inhibition of TG-induced cell death in MDA-MB-468 cells expressing p35 suggests that ICE-like protease activity is essential for apoptosis induction by TG. Although p35 mRNA expression in transfected cells was detected by RT-PCR, p35 protein was not detected (data not shown). This is consistent with earlier data indicating that low level p35 expression is sufficient to inhibit apoptosis (Hershberger et al., 1994). Moreover, inhibition of ICE-like proteases by p35 involves p35 cleavage, reducing the level of intact p35 protein available for detection by Western blotting (Bump et al., 1995; Xue and Horvitz, 1995).

A second type of evidence for involvement of ICE-like proteases in TG-induced apoptosis is the inhibition observed in cells exposed to Z-VAD-fmk. The use of this reagent to confirm the role of ICE-like proteases in mediating apoptosis in response to several different signals has been reported previously (Zhu et al., 1995; Jacobson et al., 1996). It is important to note that the concentration of Z-VAD-fmk employed in our experiments, although in the micromolar range, did not repress cell growth or decrease cell viability, whereas a control peptide fluoromethylketone, Z-FA-fmk, was toxic to cells.

In summary, the findings of the present study indicate that TG induces apoptosis of MDA-MB-468 cells, mediated through a highly conserved, Bcl-2-regulated process that involves ICE-like proteases. This model system should be useful for further investigation directed toward understanding the role of calcium in apoptosis signaling, and its relationship to Bcl-2 and the ICE-like proteolytic cascade.

1994; Furuya et al., 1994). Also, it is possible that ER calcium pool depletion may trigger apoptosis, a concept that is both supported by experimental evidence (Reynolds and Eastman, 1996) and consistent with the fact that the ER calcium pool is essential for a number of vital cellular functions, including protein processing (Lodish et al., 1992), signal transduction (Schonthal et al., 1991; Little and Lee, 1995), and cell division (Short et al., 1993). Because Bcl-2 is associated with the ER/perinuclear membrane, in addition to the outer mitochondrial membrane, we suggested the possibility that Bcl-2 might inhibit apoptosis by regulating calcium fluxes across intracellular mem-

Materials and methods

Materials

TG was purchased from LC Laboratories and serum from Hyclone. Antibiotics were from Gibco BRL. Benzylox-ycarbonyl-Val-Ala-Asp (O-methyl)-fluoromethylketone (Z-Val-Ala-Asp (O-Me)-CH$_2$F; Z-VAD-fmk) and benzylox-ycarbonyl-Phe-Ala-fluoromethylketone (Z-Phe-Ala-fmk; Z-FA-fmk) were from Enzyme Systems Products, Inc. All other chemicals, unless noted otherwise, were obtained from Sigma. Monoclonal antibody to human pro-caspase-3 was from Transduction Laboratories.

Cell Culture and Treatment Conditions

MDA-MB-468 human breast cancer cells (from M Lippman, Georgetown University) were cultured in Improved Minimal

Essential Medium (Biofluids) supplemented with 10% (v/v) heat-inactivated fetal bovine serum, 50 units/ml penicillin and 50 μg/ml streptomycin at 37°C in a 7% CO_2 atmosphere.

A 1 mg/ml stock of TG was made in DMSO and stored in aliquots at -20°C. A working stock was prepared by diluting TG in fresh culture medium to a final concentration of 1 μM. TG was then added to the cell cultures to achieve the desired final concentrations as noted in the text. Untreated cultures received the same volumes of DMSO without TG. Z-FA-fmk and Z-VAD-fmk were dissolved in DMSO to give a final concentration of 50 mM and added to 1 ml culture wells at a final concentration of 100 or 200 μM respectively 1 h before adding TG and every 12 h thereafter for a total of four additions.

Cell viability and apoptosis assays

Cells were counted on a hemocytometer after suspension in trypan blue dye. Viability was defined by the ability of cells to exclude trypan blue dye. Apoptotic cells were detected by fluorescence microscopy, using a previously published method (McCormick et al., 1997). Briefly, five million cells were gently pelleted and resuspended in 0.2 ml tissue culture medium and both ethidium bromide and acridine orange were added from 100 μg/ml stock solutions to achieve 4 μg/ml final concentrations of each. Cells were examined under a glass coverslip with u.v. illumination using a Nikon Optiphot microscope and cells were scored as apoptotic according to nuclear morphological changes, including chromatin condensation and apoptotic body formation.

Western blotting

Levels of Bcl-2 in cell lysates were measured by Western blotting as described previously using the 15131A monoclonal antibody (PharMingen) (Lam et al., 1994). To assess the level of caspase-3 at various time points after treatment with 100 nM TG, cells were washed twice with ice cold phosphate buffered saline and then lysed for 40 min in RIPA buffer (50 mM Tris-HCl, pH 7.6, 150 mM NaCl, 1% triton-X-100, 0.1% SDS, 1 mM PMSF, 1 μg/ml leupeptin). The lysates were centrifuged in a microfuge at 13 200 r.p.m. for 10 min at 4°C, the supernatants collected and the protein concentrations determined by the Bio-Rad Protein Assay (Bio-Rad Laboratories, Hercules, California). Thirty μg of each protein lysate was resolved by electrophoresis on a 14% SDS-polyacrylamide gel under reducing conditions, and transferred to PVDF membrane (Millepore Co., Bedford, Massachusetts). The membranes were incubated in 5% non-fat dry milk in T-TBS (18 mM Tris-HCl, pH 7.6, 122 mM NaCl, 0.1% Tween-20) at room temperature for 2 h and then incubated with monoclonal antibody to human caspase-3.

(Transduction Laboratories, Lexington, Kentucky) at 1:1000 dilution at 4°C for 18 h, followed by goat anti-rabbit IgG conjugated with horseradish peroxidase (GIBCO BRL, Gaithersburg, Maryland). The immune complexes were detected with the ECL Western blotting detection reagents (Amersham Corporation, Arlington Heights, Illinois) according to the manufacturer's protocol, followed by exposure to X-ray film (Sigma, St Louis, Missouri).

Vector construction and transfection

MDA-MB-468 cells were transfected by the calcium phosphate method (GIBCO/BRL Calcium Phosphate Transfection System) with the pSFFV-Bcl-2 expression vector, described previously (Cuende et al., 1993). Stable transfectants were isolated by resistance to G418. The full length cDNA encoding baculovirus p35 (P Friesen) was cloned in the sense direction into the pSFFV-neo vector (G Nunez), producing pSFFV-p35. MDA-MB-468 cells were transfected with either pSFFV-neo or pSFFV-p35 by the calcium phosphate method and stably transfected, G418-resistant, clones were isolated.

Northern blotting

Total cellular RNA was prepared using TRIZOL Reagent (GIBCO BRL). Thirty μg RNA per sample was separated by electrophoresis in a 1.2% agarose gel and blotted onto a nitrocellulose membrane. The blot was prehybridized at 65°C for 30 min and hybridized with α-^{32}P-dCTP-labeled (Stratagene Prime-It II Kit) plasmid pPRM-35K-ORF containing the full length cDNA for baculovirus p35 (Hershberger et al., 1994).

References

Armstrong DK, Isaacs JT, Ottaviano YL and Davidson NE. (1992). Cancer Res., 52, 3418–3424.
Armstrong DK, Kaufmann SH, Ottaviano YL, Furuya U, Buckley JA, Isaacs JT and Davidson NE. (1994). Cancer Res., 54, 5280–5283.
Beidler DR, Tewari M, Friesen PD, Poirier G and Dixit VM. (1995). J. Biol. Chem., 270, 16526–16528.
Bump NJ, Hackett M, Hugunin M, Seshagiri S, Brady K, Chen P, Ferenz C, Franklin S, Ghayur T, Li P, Licari P, Mankovich J, Shi L, Greenberg AH, Miller LK and Wong WW. (1995). Science, 269, 1885–1888.
Cartier JL, Hershberger PA and Friesen PD. (1994). J. Virol., 68, 7728–7737.
Chinnaiyan AM, Orth K, O'Rourke K, Duan H, Poirier GG and Dixit VM. (1996). J. Biol. Chem., 271, 4573–4576.
Cory S. (1995). Ann. Rev. Immunol., 13, 513–543.
Cuende E, Ales-Martinez JE, Ding L, Gonzalez-Garcia M, Martinez-A C and Nunez G. (1993). EMBO J., 12, 1555–1560.

Fraser A and Evan G. (1996). Cell, 85, 781–784.
Furuya Y, Lundmo P, Short AD, Gill DL and Isaacs JT. (1994). Cancer Res., 54, 6167–6175.
Ghosh TK, Bian J, Short AD, Rybak SL and Gill DL. (1989). J. Biol. Chem., 266, 24690–24697.
Hay BA, Wolff T and Rubin GM. (1994). Develop, 120, 2121–2129.
Henkart PA. (1996). Cell, 4, 195–201.
Hershberger PA, LaCount DJ and Friesen PD. (1994). J. Virol., 68, 3467–3477.
Jacobson MD, Weil M and Raff MC. (1996). J. Cell Biol., 133, 1041–1051.
Jiang S, Chow SC, Nicotera P and Orrenius S. (1994). Exp. Cell. Res., 212, 84–92.
Lam, M, Dubyak G, Chen L, Nuñez G, Miesfeld RL and Distelhorst CW. (1994). Proc. Natl. Acad. Sci. USA, 91, 6569–6573.
Lam M, Dubyak G and Distelhorst CW. (1993). Mol. Endocrinol., 7, 686–693.

Li WW, Alexandre S, Cao X and Lee AS. (1993). *J. Biol. Chem.*, **268**, 12003–12009.

Little E and Lee AS. (1995). *J. Biol. Chem.*, **270**, 9526–9534.

Lodish HF, Kong N and Wikstrom L. (1992). *J. Biol. Chem.*, **267**, 12753–12760.

Martin SJ, Amarante-Mendes GP, Shi L, Chuang T-S, Casiano CA, O'Brien GA, Fitzgerald P, Tan EM, Bokoch GM, Greenberg AH and Green DR. (1996). *EMBO J.*, **15**, 2407–2416.

Martin SJ and Green DR. (1995). *Cell*, **82**, 349–352.

McCloskey DE, Armstrong DK, Jackisch C and Davidson NE. (1996). *Rec. Prog. Horm. Res.*, **51**, 493–508.

McCormick TS, McColl KS and Distelhorst CW. (1997). *J. Biol. Chem.*, **272**, 6087–6092.

Milligan CE, Prevette D, Yaginuma H, Homma S, Cardwell C, Fritz LC, Tomaselli KJ, Oppenheim RW and Schwartz LM. (1995). *Neuron*, **15**, 385–393.

Muchmore SW, Sattler M, Liang H, Meadows RP, Harlan JE, Yoon HS, Nettesheim D, Chang BS, Thompson CB, Wong S-L, Ng S-C and Fesik SW. (1996). *Nature*, **381**, 335–341.

Rabizadeh S, LaCount DJ, Friesen PD and Bredesen DE. (1993). *J. Neurochemistry*, **61**, 2318–2321.

Reynolds JE and Eastman A. (1996). *J. Biol. Chem.*, **271**, 27739–27743.

Schonthal A, Sugarman J, Brown JH, Hanley MR and Feramisco JR. (1991). *Proc. Natl. Acad. Sci. USA*, **88**, 7096–7100.

Shimizu S, Eguchi Y, Kamiike W, Matsuda H and Tsujimoto Y. (1996). *Oncogene*, **12**, 2251–2257.

Short AD, Bian J, Ghosh TK, Waldron RT and Rybak SL. (1993). *Proc. Natl. Acad. Sci. USA*, **90**, 4986–4990.

Steller H. (1995). *Science*, **267**, 1445–1449.

Sugimoto A, Friesen PD and Rothman JH. (1994). *EMBO J.*, **13**, 2023–2028.

Thastrup O, Cullen PJ, Drobak BK, Hanley MR and Dawson AP. (1990). *Proc. Natl. Acad. Sci. USA*, **87**, 2466–2470.

Thompson CB. (1995). *Science*, **267**, 1456–1462.

Waldron RT, Short AD and Gill DL. (1995). *J. Biol. Chem.*, **270**, 11955–11961.

Xue D and Horvitz HR. (1995). *Nature*, **377**, 248–251.

Yuan J, Shaham S, Ledoux S, Ellis HM and Horvitz HR. (1993). *Cell*, **75**, 641–652.

Zhu H, Fearnhead HO and Cohen GM. (1995). *FEBS Lett.*, **374**, 303–308.